RAS Techniques and Instruments

RASTI **4,** 1–22 (2025) https://doi.org/10.1093/rasti/rzaf020
Advance Access publication 2025 May 31

ExoPhoto: a data base of temperature-dependent photodissociation cross-sections

Qing-He Ni,[1] Christian Hill,[2] Sergei N. Yurchenko ,[1] Marco Pezzella,[3] Alexander Fateev,[4] Zhi Qin ,[5] Olivia Venot [6] and Jonathan Tennyson [1]★

[1]*Department of Physics and Astronomy, University College London, Gower Street, London WC1E 6BT, UK*
[2]*International Atomic Energy Agency, Vienna A-1400, Austria*
[3]*Dipartimento di Fisica e Geologia, Universitá di Perugia, Via Alessandro Pascoli, 06123 PG, Perugia, Italy*
[4]*Department of Chemical and Biochemical Engineering, Technical University of Denmark, Søltofts Plads 229, Kgs. Lyngby DK 2800, Denmark*
[5]*School of Energy and Power Engineering, Shandong University, Jinan 250061, China*
[6]*Université Paris Cité and Univ Paris Est Creteil, CNRS, LISA, F-75013 Paris, France*

Accepted 2025 May 28. Received 2025 May 18; in original form 2024 December 29

ABSTRACT

We present the ExoPhoto data base www.exomol.com/exophoto, an extension of the ExoMol data base, specifically developed to address the growing need for high-accuracy, temperature-dependent photodissociation cross-section data towards short-UV wavelengths. ExoPhoto combines theoretical models from three major computational data bases (ExoMol, UGAMOP and PhoMol) and experimental data sets from two experimental groups, providing extensive wavelength and temperature coverage. ExoPhoto currently includes photodissociation data for 20 molecules: AlH, HCl, HF, MgH, OH, NaO, MgO, O_2, AlCl, AlF, CS, HeH^+, CO, CO_2, H_2O, SO_2, C_2H_2, C_2H_4, H_2CO, and NH_3, derived from theoretical models and supported by experimental data from 5 data bases.

ExoPhoto also includes detailed data on branching ratios and quantum yields for selected data sets. The data structure of ExoPhoto follows the ExoMol framework, with a consistent naming convention and hierarchical JSON-based organization. Photodissociation cross sections are stored in a set of `.photo` files which provide data as a function of wavelength with one file for each target molecule temperature. Future developments aim to include more photodissociation cross section data and to provide data for molecules in non-local thermodynamic equilibrium (non-LTE). These will expand the utility of ExoPhoto for advanced astrophysical, planetary modeling and industrial applications.

Key words: Data Methods – ExoMol – Photodissociation – Database.

1 INTRODUCTION

Photodissociation is the process in which chemical bonds are broken due to the absorption of one or more photons. This is a very important process in astronomy because the chemistry of upper planetary atmospheres, as in case of the Earth's atmosphere, and the interstellar medium is heavily reliant on photodissociation. Molecular temperature can have a significant impact on the photodissociation rate since rising temperatures increase the number of vibrationally excited states populated and therefore decrease the photodissociation threshold (Stibbe & Tennyson 1998). As a result, the photodissociation rates in exoplanets orbiting close to cooler stars can rise rapidly at molecular temperatures beyond 1000 K, but the details of this behaviour depends strongly on the radiation fields (Schinke 1993; Pezzella et al. 2022). An important aspect in the evolution of the atmospheres of exoplanets is photon-initiated chemistry. In this phenomenon, the composition and dynamics of the atmosphere for planets orbiting stars in ultraviolet (UV) rich environments caused by high-energy photons are dominated by photodissociation (Venot et al. 2016; Badhan et al. 2019; Fleury et al. 2019; Lewis et al. 2020).

In recent years, photodissociation data bases have become a critical resource for exploring molecular interactions under UV radiation, with applications spanning planetary atmospheres to interstellar environments. The Leiden data base (Heays et al. 2017; Hrodmarsson & Van Dishoeck 2023), established in the 1980s, has served as a cornerstone for astrochemical modelling, particularly for studies involving interstellar media (ISM) and photon-dominated regions (PDRs). This data base compiles the essential molecular data required to calculate photodestruction rates in various astrophysical contexts. It is constructed based on laboratory and theoretical data sets, ensuring the inclusion of species with verified cross-section data. Currently, it features cross-sections for 116 atoms and molecules covering photoabsorption, photonionization and, for molecules, photodissociation, with no temperature dependence indicated and a tacit assumptions that the molecules are cold.

The MPI-Mainz UV/VIS Spectral Atlas (Keller-Rudek et al. 2013), initially developed in the early 1980s and made available online in 2003, provides one of the most extensive data sets for atmospheric research, covering nearly a century of mainly experimental

★ E-mail: j.tennyson@ucl.ac.uk

studies. With data for approximately 900 species, it includes UV and visible absorption cross-sections and quantum yields, totaling over 5500 cross-section files. While it offers extensive UV and visible absorption cross-sections, the data provided is largely recorded at room temperature. These resources are vital for understanding kinetic and photochemical processes in atmospheric chemistry. Building upon this, the VAMDC (Virtual Atomic and Molecular Data Centre) (Dubernet et al. 2016; Albert et al. 2020), integrates the MPI-MAINZ data base within its unified e-science framework, enabling seamless access to photodissociation data from multiple sources through a single interface.

The UGAMOP data base (University of Georgia Molecular Opacity Project) (UGA 2014) was designed to address astrophysical needs for accurate line and continuum opacity data. It features calculated temperature-dependent photodissociation cross-sections for four molecules: CS (Pattillo et al. 2018), H_2 (Gay et al. 2012), HeH^+ (Miyake et al. 2011), and MgH (Weck et al. 2003c, a, b). The photodissociation cross-sections for CS, H_2, HeH^+, and MgH, all assume local thermodyamic equilibrium (LTE), while for H_2 non-LTE is also allowed but not all photodissociaiton pathways are considered. These data sets are particularly significant for modelling extrasolar giant planets (EGPs) and cool stellar atmospheres.

In 2014, PHIDRATES (PhotoIonization and Dissociation Rates for Atmospheric and Terrestrial Environments) (Huebner & Mukherjee 2015) was introduced, providing detailed photoionization and photodissociation rates. This data base supports studies involving solar and blackbody radiation fields and is particularly useful for comet modelling, planetary atmospheres, and heliospheric dynamics. Rate coefficients for ionization and dissociation have been determined for more than 140 atoms, molecules, and ions within radiation fields generated by both the quiet and active Sun at a heliocentric distance of 1 AU, as well as from black bodies characterized by selected temperatures spanning from 1000 K to 10^6 K, without considering any radiation dilution due to the distance from these sources or the dependence on the temperature of molecular species.

The MOL-D data base (Vujčič et al. 2015), hosted by the Belgrade Astronomical Observatory since 2015, focuses on temperature-independent photodissociation cross-sections for ro-vibrational states of molecular ions, including He_2^+, H_2^+, and LiH^+. As part of the Serbian Virtual Observatory (SERVO) and VAMDC, this data base offers cross-section data and rate coefficients for specific collisional processes, accessible via a user-friendly web interface.

Since 2017, the Metal Oxides Photolysis data base (Valiev et al. 2017), has provided quantum chemistry-based photolysis cross-sections for molecules like LiO, NaO, and MgO focusing on high-temperature environments, although the cross-sections provided are not actually temperature-dependent. These data sets are crucial for studying planetary exospheres, as photolysis of metal oxides contributes to the release of metal atoms, impacting observations of exospheric dynamics.

Recently, a photodissociation cross-section project called PHOMOL has been initiated by a research team at the School of Energy and Power Engineering, Shandong University in China which has computed temperature-dependent cross-sections for a range of astrophysically important diatomic molecules, including, AlCl (Qin et al. 2021a), AlF (Qin et al. 2022a), AlH (Qin et al. 2021b), HCl (Qin et al. 2022b), HF (Qin, Bai, & Liu 2022b), MgO (Bai et al. 2021), NaO (Bai et al. 2023), and O_2 (Qin et al. 2023). These photodissociation cross-sections are considered further below.

Together, these data bases and data sets form a network of resources, enabling simulations of molecular behaviour in diverse radiation environments and advancing our understanding of astrophysical, atmospheric, and industrial photochemistry.

The EXOMOL project was originally established to provide extensive, temperature-dependent spectroscopic data sets involving bound-bound transitions (Tennyson & Yurchenko 2012). However, modellers also need information on dissociative processes as this often drives chemistry.

To address this issue, the EXOMOL project is undertaking a significant expansion of its data base (www.exomol.com) to consider processes at ultraviolet wavelengths including continuum absorption (Yurchenko et al. 2024), pre-dissociation (Mitev et al. 2024; Yurchenko et al. 2024; Mitev et al. 2025a) and photodissociation (Pezzella et al. 2021, 2022, 2024). At present, the EXOMOL data base is largely a molecular line lists data base that can be used to simulate photo-absorption and radiative transfer in astrophysical environments such as exoplanets, brown dwarfs, cold stars, and sunspots and characterize their spectral properties. Extensive line lists are the basis of the data base (Tennyson et al. 2024); they are then complemented with state lifetimes, dipoles, Landé g-factors, cooling functions, temperature-dependent cross-sections, opacity functions, specific heats etc. Due to their completeness as a function of frequency and their coverage of molecular species, and, most critically, temperature, EXOMOL data are widely used by astronomers studying exoplanet and other objects.

The EXOPHOTO data base extends the EXOMOL data base by providing photodissociation cross-section data extracted from EXOMOL and other data bases. Specifically, EXOPHOTO draws its photodissociation cross-sections and branching ratios directly from the primary data-producing the EXOMOL project, the PHOMOL Team, and the UGAMOP data base with experimental data from Danish Technical University (DTU, published here for the first time) and the EXACT (EXoplanetary Atmospheric Chemistry at High Temperature) data base (Venot O. et al. 2024).

EXOPHOTO aims to compile temperature-dependent photodissociation cross-section data for molecules relevant to astrophysics, filling gaps identified in the literature, particularly with regards to temperature-dependence. By providing a unified format for photodissociation cross-section data, this initiative simplifies the process for scientists to reliably compute photodissociation rates and model photon-rich environments, such as the top of exoplanetary atmospheres.

2 DATA BASE COVERAGE

The goal of the EXOMOL project is to include all of the spectroscopic characteristics of molecules that are thought to be significant in hot astrophysical environments. To a certain degree, the required temperature and frequency range completeness depend on what is needed for astronomical and other research such as combustion studies.

Table 1 list molecules for which the EXOPHOTO data base currently provides data taken from calculations or measurements, respectively. These data sets are either already freely available in the literature or have been provided directly to us for inclusion in the EXOPHOTO data base. The calculated data summarized in Table 1 have been obtained by the EXOMOL, UGAMOP and PHOMOL groups. The experimental data given in Table 1 have been taken from the work of Venot et al. (2018), Fleury et al. (2025), see the EXACT data base (Venot O. et al. 2024), and studies performed at the Danish Technical University (DTU) by Fateev and co-workers. Note that these experiments actually measure UV photoabsorption cross-sections rather than explicit photodissociation cross-sections;

Table 1. Summary of calculated and experimental photodissociation cross-section data in the ExoPhoto data base

Data type	ID	Molecule	Isotopologue	Data set	N_{files}	Temperature Range (K)	Wavelength Range (nm)	Pressure Range (bar)	Reference
Calculated	1	AlH	$^{1}H^{27}Al$	PhoMol	209	100–10 450	50–1000.1	0	Qin, Bai, & Liu (2021b)
	2	HCl	$^{1}H^{35}Cl$	PTY	34	0.01–10 000	100–400	0	Pezzella, Yurchenko, & Tennyson (2022)
	3			PhoMol	34	0.01–10 000	50–500	0	Qin, Bai, & Liu (2022b)
	4	HCl	$^{1}H^{37}Cl$	PTY	34	0.01–10 000	100–400	0	Pezzella, Yurchenko, & Tennyson (2022)
	5		$^{2}H^{35}Cl$	PTY	34	0.01–10 000	100–400	0	Pezzella, Yurchenko, & Tennyson (2022)
	6		$^{2}H^{37}Cl$	PTY	34	0.01–10 000	100–400	0	Pezzella, Yurchenko, & Tennyson (2022)
	7	HF	$^{1}H^{19}F$	PTY	34	0.01–10 000	90–400.1	0	Pezzella, Yurchenko, & Tennyson (2022)
	8			PhoMol	34	0.01–10 000	50-500	0	Qin, Bai, & Liu (2022b)
	9		$^{2}H^{19}F$	PTY	34	0.01–10 000	90-400.1	0	Pezzella, Yurchenko, & Tennyson (2022)
	10	MgH	$^{24}Mg^{1}H$	UGAMOP	10	1000–10 000	170-454	0	Weck, Stancil, & Kirby (2003c), Weck et al. (2003a), Weck et al. (2003b)
	11	OH	$^{16}O^{1}H$	MYTHOS	80	0.01–7900	82.8–2000	0	Mitev et al. (2025b)
	12	NaO	$^{23}Na^{16}O$	PhoMol	34	0.01–10 000	50–500	0	Bai et al. (2023)
	13	MgO	$^{24}Mg^{16}O$	PhoMol	35	0.01–10 000	50–1000.1	0	Bai et al. (2021)
	14	O_2	$^{16}O^{16}O$	PhoMol	101	0–10 000	50–500	0	Qin et al. (2023)
	15	AlCl	$^{27}Al^{35}Cl$	PhoMol	201	0.01–10 000	50–499	0	Qin, Bai, & Liu (2021a)
	16	AlF	$^{27}Al^{19}F$	PhoMol	201	0.01–10000	50–1000.1	0	Qin, Bai, & Liu (2022a)
	17	CS	$^{12}C^{32}S$	UGAMOP	10	1000–10 000	50–5000	0	Pattillo et al. (2018)
	18	HeH^+	$^{1}H\,^{4}He$	UGAMOP	9	500–12 000	10–112.7	0	Miyake, Gay, & Stancil (2011)
Experimental	19	CO	–	DTU	2	305–1630	117.04–228.8	1–1.0658	–
	20	CO_2	–	DTU	5	305–1630	108.79–323.79	1–1.0647	–
	21	CO_2	–	EXACT	9	150–800	114–230	1	Venot et al. (2018)
	22	H_2O	–	DTU	5	423.15–1773.15	108.81–236.81	1	–
	23	SO_2	–	DTU	1	423.15	110.35–230.36	1	–
	24	C_2H_2	–	photo-FPBV	6	296–773	116–228	1	Fleury et al. (2025)
	25	C_2H_4	–	DTU	1	562.15	113.29–201.25	1	–
	26	H_2CO	–	DTU	4	303.15–573.15	110–230.014	1	–
	27	NH_3	–	DTU	2	289–295.55	113.28–201.25	1	–

here, as has been done elsewhere, see Venot et al. (2018) for example, we equate these absorption cross-sections directly with photodissociation which yields an upper limit and may lead to a slight overestimation of the true photodissociation cross-section. Note that while calculated cross-sections are all for a single, specified isotopologue, the experimental data are for isotopologue mixtures in terrestrial natural abundance.

The ExoMol project has developed a specific methodology based on time-independent quantum mechanical calculations using standard bound-state nuclear motion codes to derive photodissociation cross-sections (Pezzella, Yurchenko, & Tennyson 2021; Pezzella et al. 2024). This methodology involves solving the Schrödinger equation to determine molecular energy levels, generating potential energy curves (PECs), and identifying transitions involving unbound states (Mitev et al. 2025a). For diatomic molecules, the variational nuclear-motion program Duo (Yurchenko et al. 2016) has thus been employed, while post-processing techniques involves Gaussian smoothing (Pezzella, Yurchenko, & Tennyson 2021; Pezzella et al. 2024; Uhlikova et al. 2025). We note that PhoMol and UGAMOP use more standard methods which explicitly treat the full set of continuum states; however, thus far PhoMol has not considered photodissociation resulting from pre-dissociation, which can be significant in the important long wavelength (near threshold) region for some molecules. These methodological differences should be kept in mind when comparing the ExoMol and PhoMol calculations presented below. For the experimentally obtained photodissociation data, the data sets contains some negative values, which likely arise from experimental noise or baseline errors. However, the number of negative values is overall small and removing them would have the effect of artificially raising the baseline.

2.1 Diatomics

2.1.1 AlCl (PhoMol) (Qin, Bai, & Liu 2021a)

Photodissociation cross-sections for the single isotopologue $^{27}Al^{35}Cl$ were computed with PhoMol over a wavelength range of 50–499 nm and for temperatures from 0.01 K to 10 000 K; example results at two temperatures are shown in Fig. 1. The required potential energy curves and transition dipole moments for the ground $X^1\Sigma^+$ state and six excited singlet states were obtained via HF + CASSCF/aug-cc-pV6Z followed by icMRCI+Q/aug-cc-pV6Z. State-resolved cross-sections from all 38 958 rovibrational levels were then determined by numerically solving the radial Schrödinger equation across photon wavelengths from 50 nm to the dissociation threshold.

2.1.2 AlF (PhoMol) (Qin, Bai, & Liu 2022a)

For aluminum monofluoride ($^{27}Al^{19}F$), photodissociation cross-sections were computed by the PhoMol project over the wavelength range 50.0–1000.1 nm for temperatures from 0.01 K to 10 000 K; example results at two temperatures appear in Fig. 2. Potential energy curves and transition dipole moments for the ground $X^1\Sigma^+$ state and seven excited singlet states were calculated via icMRCI+Q with the aug-cc-pCV5Z-DK basis set. State-resolved cross-sections from 36 349 rovibrational levels of the $X^1\Sigma^+$ state were then obtained by

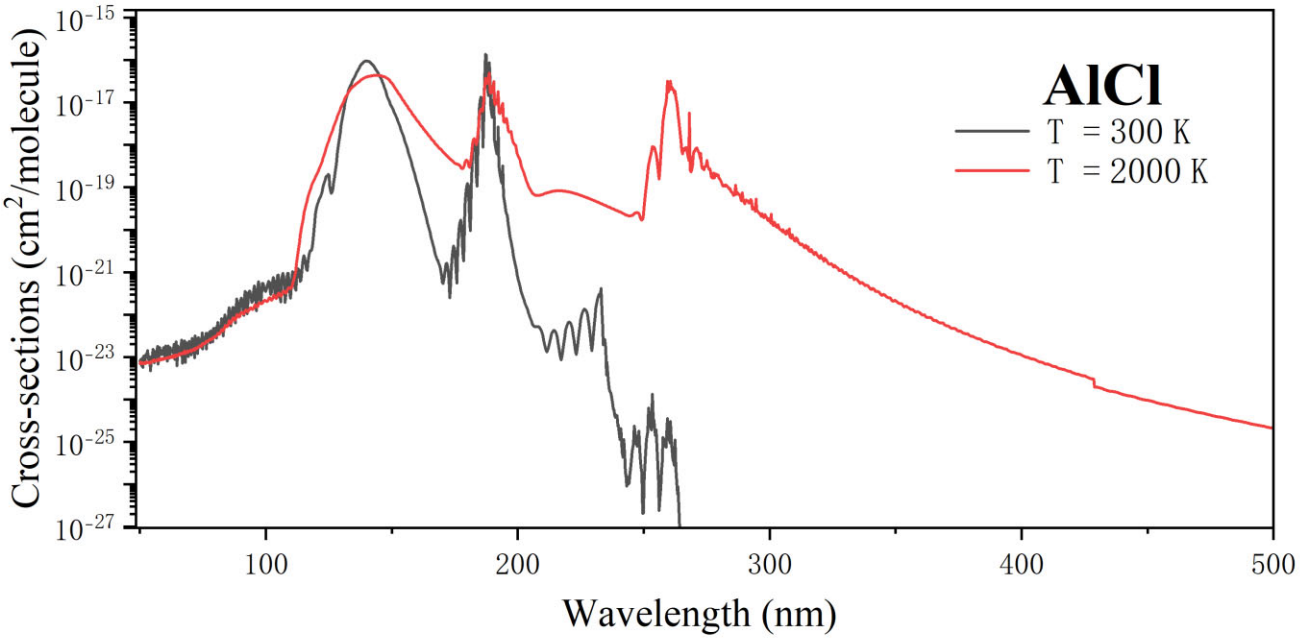

Figure 1. AlCl from PHOMOL spectrum overview (Qin, Bai, & Liu 2021a).

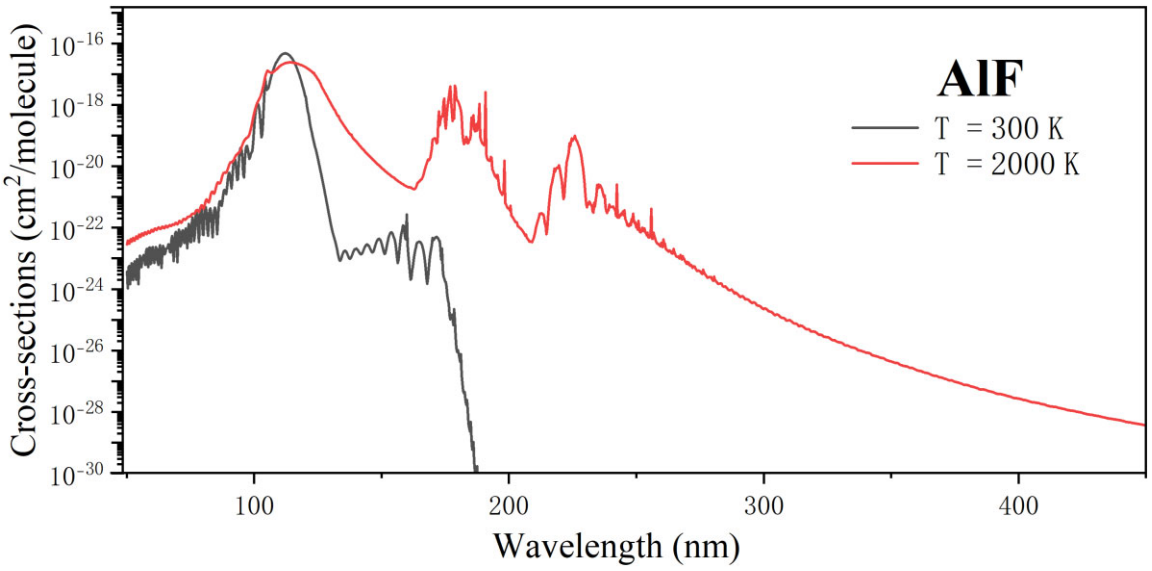

Figure 2. AlF spectrum overview from PHOMOL (Qin, Bai, & Liu 2022a).

numerically solving the continuum wavefunctions. These data have been applied to carbon-star envelope models, where AlF abundance is governed by photodissociation.

2.1.3 AlH (PhoMol) (Qin, Bai, & Liu 2021b)

The aluminum hydride ($^{27}Al^{1}H$) molecule's photodissociation cross-sections were calculated by PHOMOL, see Fig. 3. Wavelengths range from 50 to 1000.1 nm, and calculations were performed for temperatures from 100 K to 10 450 K. We note these cross-sections neglect the effects of pre-dissociation which studies have shown to be important for AlH (Pavlenko et al. 2022; Yurchenko et al. 2024) and their inclusion is likely to significantly increase the photodissociation cross-section at long wavelengths.

2.1.4 CO (DTU) (Fateev et al., private communication)

Photodissociation cross-sections for carbon monoxide (CO) were recorded in the far-UV region at the Danish Technical University (DTU) by Fateev and co-workers. The data span a wavelength range from 117.04 to 228.8 nm and are provided for two temperatures, 1630 K and 305 K, for pressures of 1 to 1.0658 bar, see Fig. 4.

2.1.5 CS (UGAMOP) (Pattillo et al. 2018)

Photodissociation cross-sections of carbon monosulfide ($^{12}C^{32}S$) were calculated using quantum-mechanical techniques by UGAMOP, see Fig. 5. Transitions were modelled from the $X\,^1\Sigma^+$ electronic ground state to six low-lying excited states ($A\,^1\Pi$, $A'\,^1\Sigma^+$,

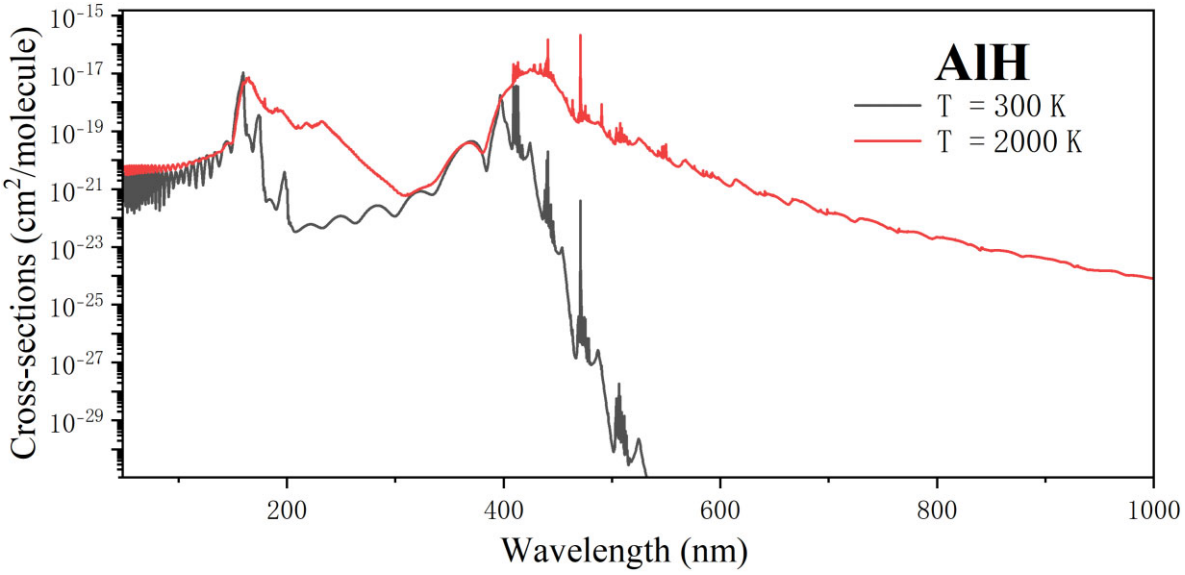

Figure 3. AlH spectrum overview (Qin, Bai, & Liu 2021b).

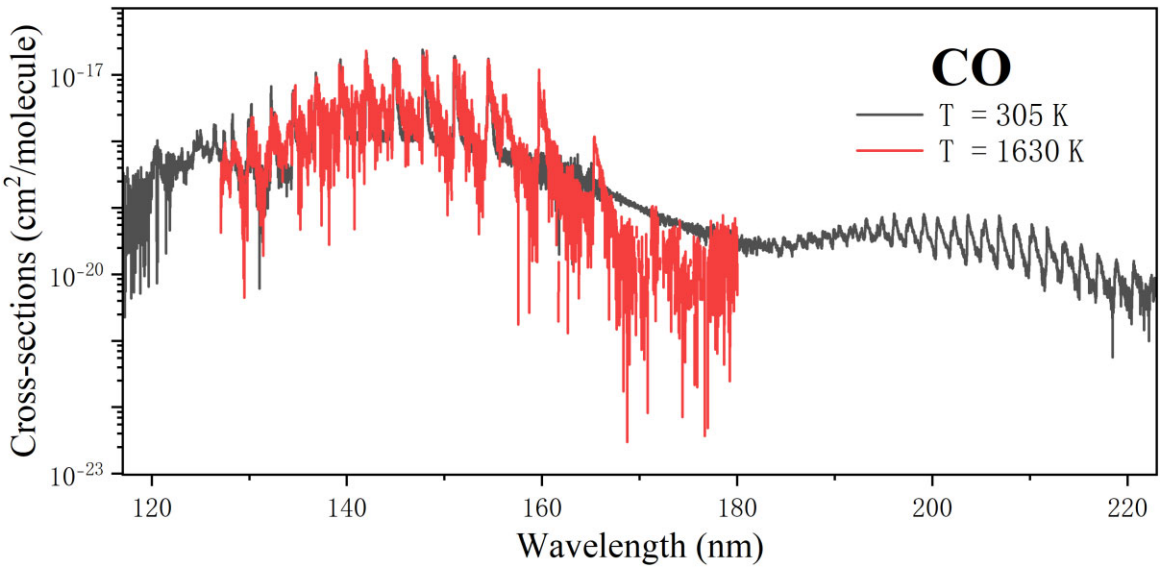

Figure 4. CO spectrum overview (Fateev et al., private communication).

$2\,^1\Pi$, $3\,^1\Pi$, $B\,^1\Sigma^+$, and $4\,^1\Pi$). Cross-sections cover a wavelength range of 50 to 5000 nm and were evaluated for temperatures between 1000 K and 10 000 K. These results provide essential insights for astrophysical applications, including dense interstellar clouds, planetary nebulae, and photodissociation regions.

2.1.6 HCl and HF (ExoMol and PhoMol) (Pezzella, Yurchenko, & Tennyson 2022; Qin, Bai, & Liu 2022b)

The ExoMol project computed photodissociation cross-sections for HCl and HF using high-accuracy potential energy curves (PECs) and dipole moment curves (DMCs) from advanced quantum mechanical methods. Calculations employed the Duo variational nuclear motion program (Yurchenko et al. 2016) to solve the Schrödinger equation for both bound and unbound states. The Gaussian-smoothed cross-sections were validated against available experimental data. These results can be used to model UV-driven processes in diverse astrophysical and planetary environments, particularly in hot and UV-rich regions.

For HCl, the ExoMol photodissociation data base (PTY) provides cross-sections for four isotopologues: $^1H^{35}Cl$, $^1H^{37}Cl$, $^2H^{35}Cl$, and $^2H^{37}Cl$. These cross-sections span a wavelength range of 100 to 400 nm and are evaluated across 34 temperatures, ranging from 0.01 K to 10 000 K. The temperature values correspond to excitation conditions of the gas, assuming local thermal equilibrium (LTE) and the Boltzmann distribution for the population of energy states. The total cross-sections were obtained by summing contributions from all final electronic states.

PhoMol also includes cross-sections for $^1H^{35}Cl$, calculated over the wavelength and temperature ranges 50 to 500 nm and 0.01 K to 10 000 K. Temperature-dependent cross-sections are evaluated across 34 temperatures.

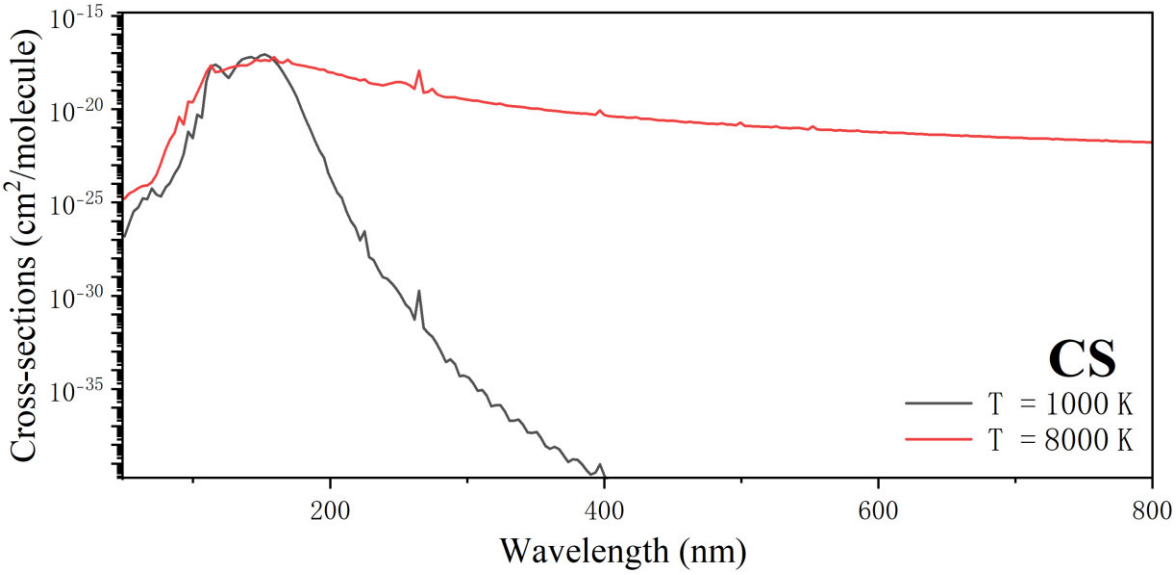

Figure 5. CS spectrum overview (Pattillo et al. 2018).

Similarly, HF photodissociation cross-sections in the ExoMol PTY data base were computed using the same methodology. The data base provides data for two isotopologues: $^{1}H^{19}F$ and $^{2}H^{19}F$. These calculations account for transitions involving both bound and unbound states, with cross-sections covering a wavelength range of 90 to 400.1 nm and evaluated over the same temperature grid (0.01 K to 10 000 K).

PhoMol also includes $^{1}H^{19}F$ data, with the 90–400.1 nm wavelength and 0.01–10 000 K temperature ranges as PTY. The data base includes seven electronic transitions with state-resolved cross sections derived from all rovibrational levels of the $X^{1}\Sigma^{+}$ state.

The ExoMol and PhoMol results for the two species are in very good agreement, see Figs 6 and 7. All the HCl isotopologue spectrum overviews from ExoMol are shown in Fig. 8. A spectrum overview for $^{1}H^{19}F$ and $^{2}H^{19}F$ isotopologues from ExoMol is shown in Fig. 9.

Both data bases provide critical cross-section data for studying photodissociation processes in interstellar and planetary environments. We therefore recommend the ExoMol data sets as these provide cross-sections for all the stable isotopologues but note that those interested in short wavelengths it will need to use the PhoMol results.

2.1.7 HeH^{+} (UGAMOP) (Miyake, Gay, & Stancil 2011)

Accurate photodissociation cross-sections for the helium hydride ion ($^{4}He^{1}H^{+}$) were calculated by UGAMOP. The calculations covered all vibrational levels ($v'' = 0$ to 11). They are illustrated in Fig. 10.

2.1.8 MgH (UGAMOP) (Weck, Stancil, & Kirby 2003c; Weck et al. 2003a, b)

Photodissociation cross-sections for $^{24}Mg^{1}H$ were calculated by UGAMOP using high-accuracy PECs and DMCs derived from a combination of *ab initio* and experimental methods. The cross-sections primarily focus on the $B'^{2}\Sigma^{+} \leftarrow X^{2}\Sigma^{+}$ and $A^{2}\Pi \leftarrow X^{2}\Sigma^{+}$ electronic transitions, covering rovibrational levels of the ground state. Cross-sections span the wavelength range from 170 to 454 nm and are provided for temperatures between 1 000 K and 10 000 K. UGAMOP cross-sections of MgH for $T = 300$ and 2000 K are illustrated in Fig. 11.

2.1.9 MgO (PhoMol) (Bai et al. 2021)

Magnesium oxide ($^{24}Mg^{16}O$) photodissociation cross-sections were computed as part of the PhoMol project for transitions from the $X^{1}\Sigma^{+}$ state. Bai et al. (2021) note that the photodissociation cross-sections from the $a^{3}\Pi$ state are questionable due to an incorrect treatment of its partition function; these cross-sections are therefore omitted here. The wavelength range covers 50–500 nm, and cross-sections were evaluated for temperatures between 0.01 K and 10 000 K; example results at two temperatures are shown in Fig. 12. As with other PhoMol data sets, this study considers only direct continuum dissociation and does not include any pre-dissociation contributions, which may be significant for MgO. These results are important for modelling magnesium chemistry in planetary exospheres and the envelopes of evolved stars.

2.1.10 NaO (PhoMol) (Bai et al. 2023)

Photodissociation cross-sections of sodium oxide ($^{23}Na^{16}O$) were computed as part of the PhoMol project for transitions from the $X^{2}\Sigma^{+}$ and $A^{2}\Sigma^{+}$ states over the wavelength range 50–500 nm and temperatures 0.01–10 000 K; example results at two temperatures are shown in Fig. 13. PECs and DMCs for the seven lowest electronic states were obtained via CASSCF followed by valence icMRCI+Q with the aug-cc-pCV6Z basis set. State-resolved cross-sections were then derived by numerically solving the nuclear Schrödinger equation across all bound rovibrational levels. However, as with other PhoMol data sets, only direct continuum dissociation is treated and pre-dissociation contributions are omitted. These data are essential for modelling sodium photochemistry in planetary exospheres and cool stellar atmospheres.

2.1.11 OH (ExoMol) (Mitev et al. 2025b)

The photodissociation cross-sections for the hydroxyl radical (OH) computed by ExoMol adopted the main features of the spectroscopic model used to compute the MYTHOS line list (Mitev et al. 2025a); this model was calculated using high-accuracy multi-reference configuration interaction (MRCI) PECs and couplings, adjusted to available experimental data (Bowesman et al. 2022) where available, and transition DMCs. The model incorporated key electronic states,

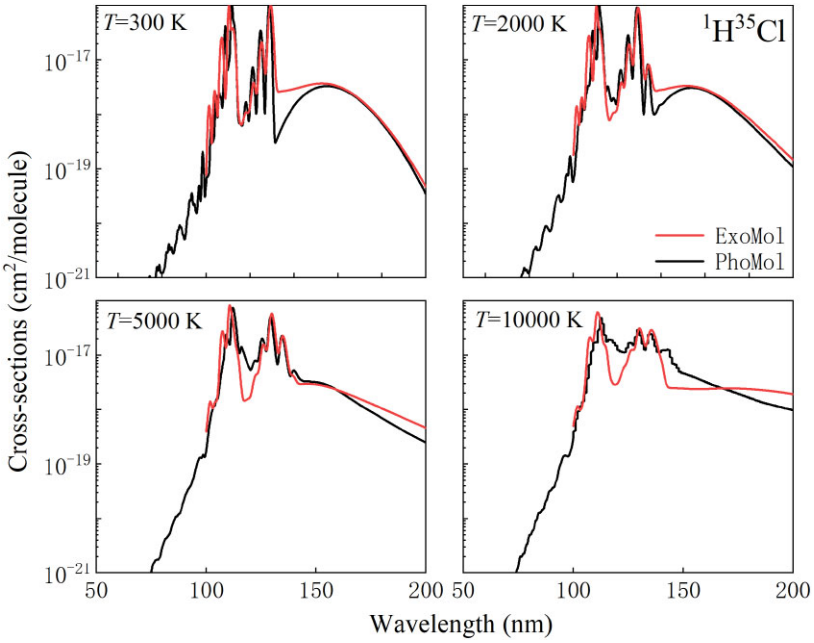

Figure 6. ^{1}H^{35}Cl spectrum overview for ExoMol and PhoMol (Pezzella, Yurchenko, & Tennyson 2022; Qin, Bai, & Liu 2022b).

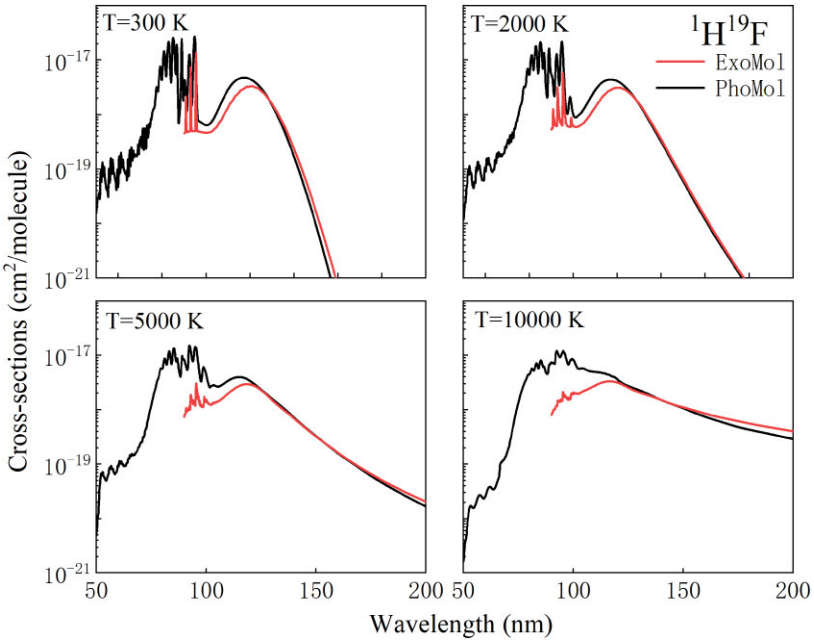

Figure 7. ^{1}H^{19}F spectrum overview for ExoMol and PhoMol (Pezzella, Yurchenko, & Tennyson 2022; Qin, Bai, & Liu 2022b).

including $X\,^2\Pi$, $A\,^2\Sigma^+$, and repulsive states such as $1\,^2\Sigma^-$, $1\,^4\Sigma^-$, and $1\,^4\Pi$ for ^{16}O^{1}H; cross-sections were computed over a wavelength range from 82.8 to 2000 nm and evaluated for 81 temperatures ranging from 0 K to 8000 K. Gaussian smoothing was applied to ensure continuous profiles, and the results were tested against cross-sections in the Leiden data base. The OH cross-sections are illustrated in Fig. 14. These cross-sections provide essential data for studying UV-driven processes in atmospheric and astrophysical environments.

We are working on extensions to the ExoPhoto data base to allow for the inclusion the photodissociation cross-sections needed for studies of non-local thermodynamic equilibrium environments, which are important for OH. At present these data are available up request to the corresponding author.

2.1.12 O_2 (PhoMol) (Qin et al. 2023)

The photodissociation cross-sections for dioxygen ($^{16}O_2$) were computed as part of the PhoMol project for photon wavelengths from 50 Å to the relevant dissociation thresholds (approximately 50–500 nm) and for gas temperatures 0–10 000 K; example results at two temperatures are shown in Fig. 15. PECs and DMCs for the four key photodissociation channels ($X^3\Sigma_g^- \rightarrow B^3\Sigma_u^-$, $X^3\Sigma_g^- \rightarrow E^3\Sigma_u^-$, $a^1\Delta_g \rightarrow {}^1\Pi_u$, $b^1\Sigma_g^+ \rightarrow 1^1\Pi_u$) were obtained at the icMRCI+Q/aug-cc-pwCV5Z-DK level, and state-resolved cross-sections were derived by numerically solving the nuclear Schrödinger equation followed by Boltzmann averaging over 0–10 000 K.

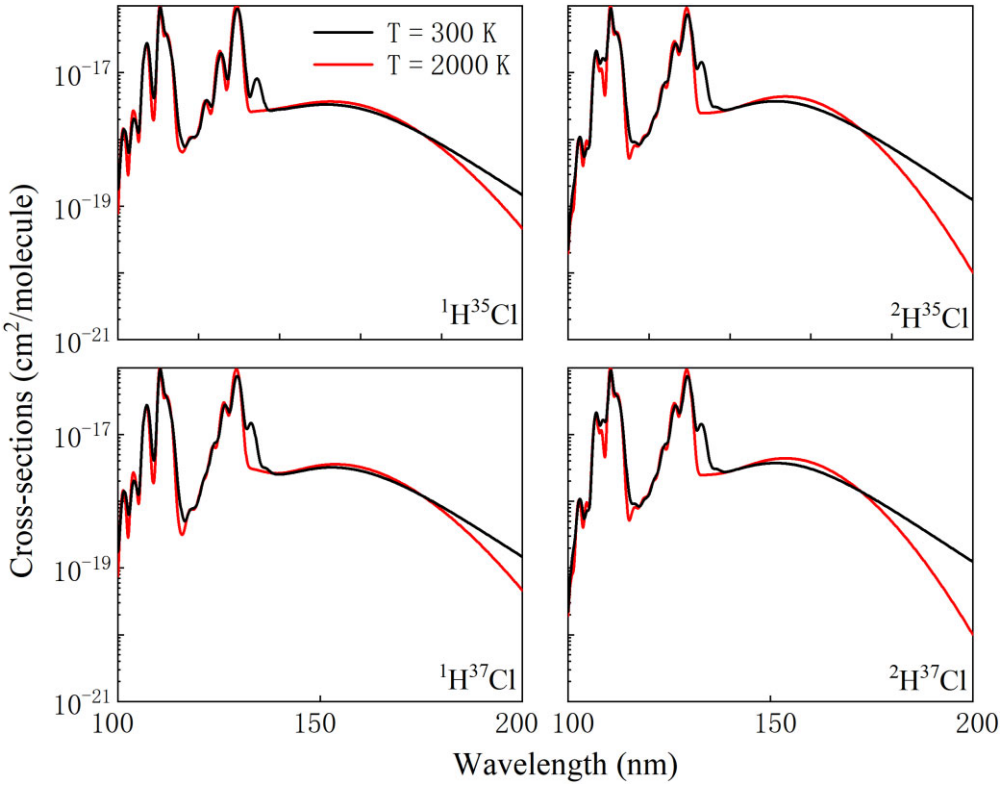

Figure 8. HCl spectrum overview for ExoMol (Pezzella, Yurchenko, & Tennyson 2022).

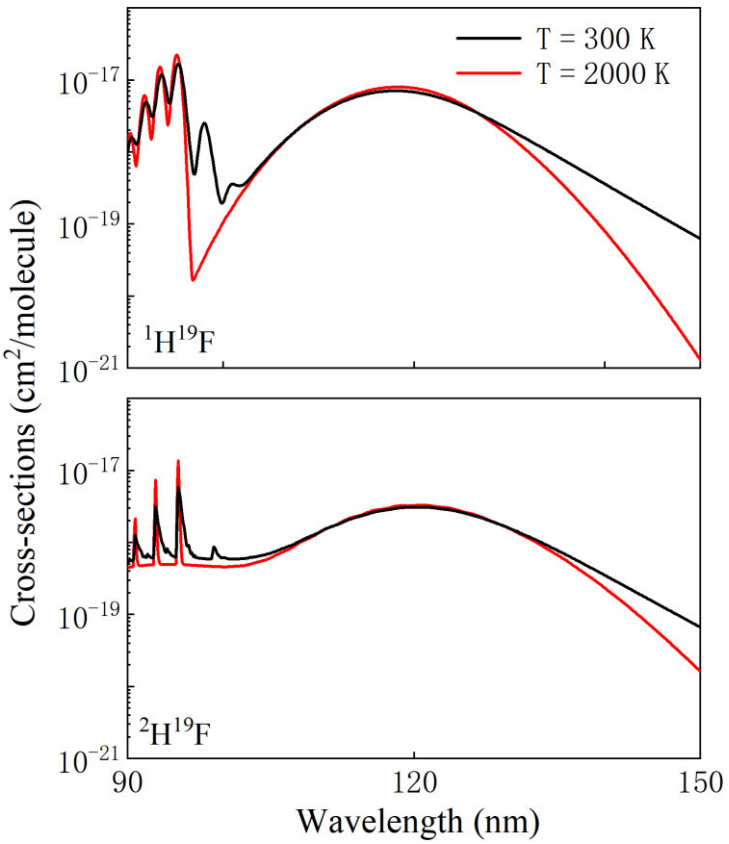

Figure 9. HF spectrum overview from ExoMol (Pezzella, Yurchenko, & Tennyson 2022).

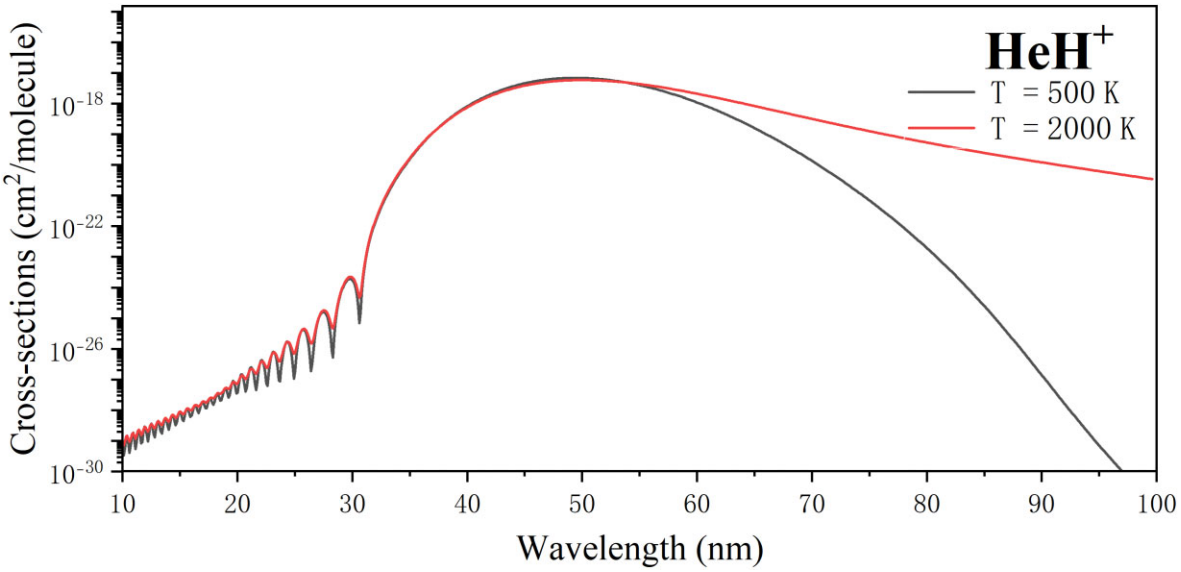

Figure 10. HeH^+ spectrum overview (Miyake, Gay, & Stancil 2011).

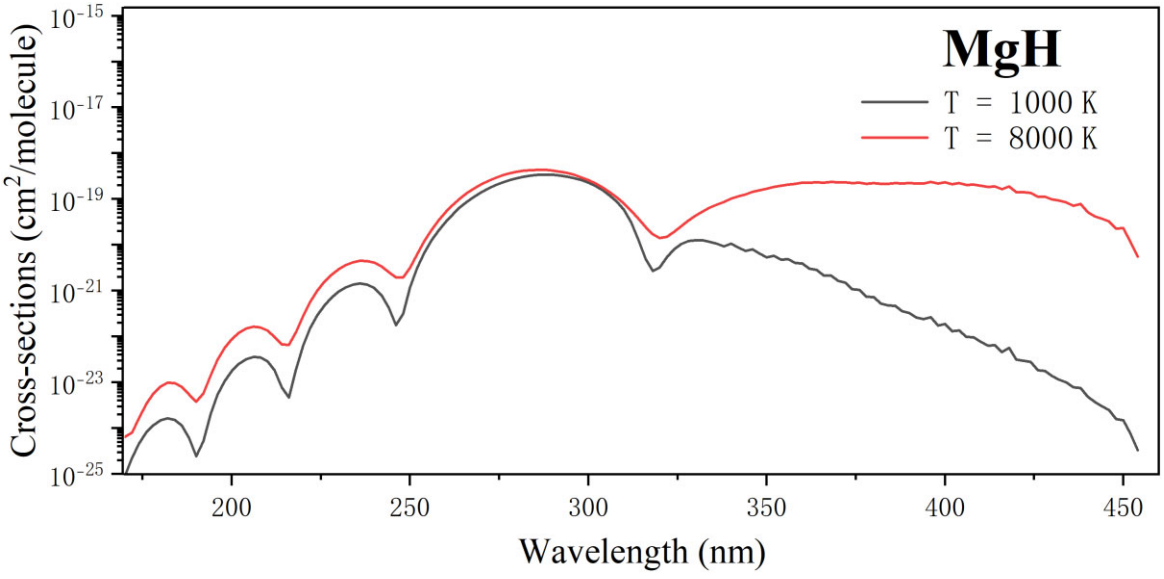

Figure 11. MgH spectrum overview (Weck, Stancil, & Kirby 2003c; Weck et al. 2003a, b).

2.2 Triatomics

2.2.1 CO_2 (DTU and EXACT) (Venot et al. 2018; Fateev et al., private communication)

The ExoPhoto data base provides two comprehensive data sets offering temperature- and pressure-dependent absorption properties for CO_2.

Photodissociation cross-sections for carbon dioxide (CO_2) measured by DTU and EXACT data bases, see Fig. 16. Data from DTU span a wavelength range of 108.79–323.79 nm with a resolution of 0.01 nm, covering a temperature range from 305 K to 1630 K for pressures of 1 to 1.0647 bar. The measurements include cross-sections at 305 K for wavelengths between 119.367 and 189.947 nm, at 550 K for wavelengths from 120.950 to 213.870 nm at 1.0647 bar, and at 1630 K for wavelengths extending from 122.420 nm up to 279.612 nm.

The EXACT data base also provides complementary data for a wavelength range of 114–230 nm with a resolution of 0.03 nm, covering temperatures from 150 K to 800 K under the pressure of 1 bar.

2.2.2 H_2O (DTU)(Fateev et al., private communication)

Photodissociation cross-sections for water (H_2O) were experimentally measured by DTU in the far-UV range. The cross-sections span multiple wavelength ranges and resolutions, depending on the temperature. For temperatures of 423.15 K and 573.15 K, the wavelength range is 110–230 nm, with a resolution of 0.015 nm. At higher temperatures of 1630 K and 1773.15 K, the wavelength ranges extend to 108–237 and 182–231 nm, with a finer resolution of 0.010 nm under pressure of 1 bar, see Fig. 17.

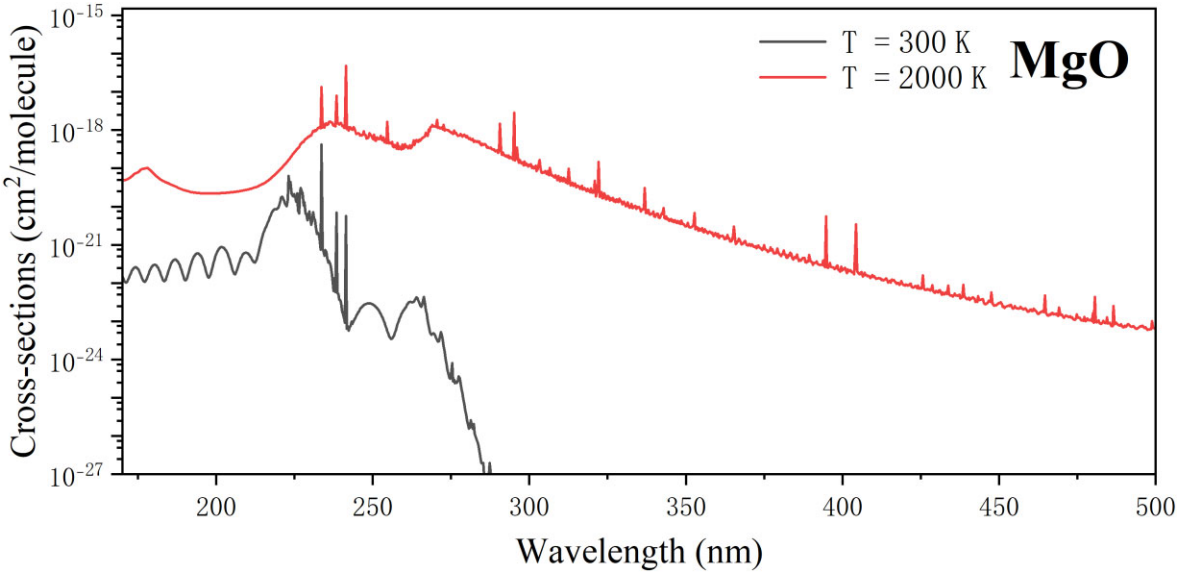

Figure 12. MgO photodissociation cross-sections (Bai et al. 2021).

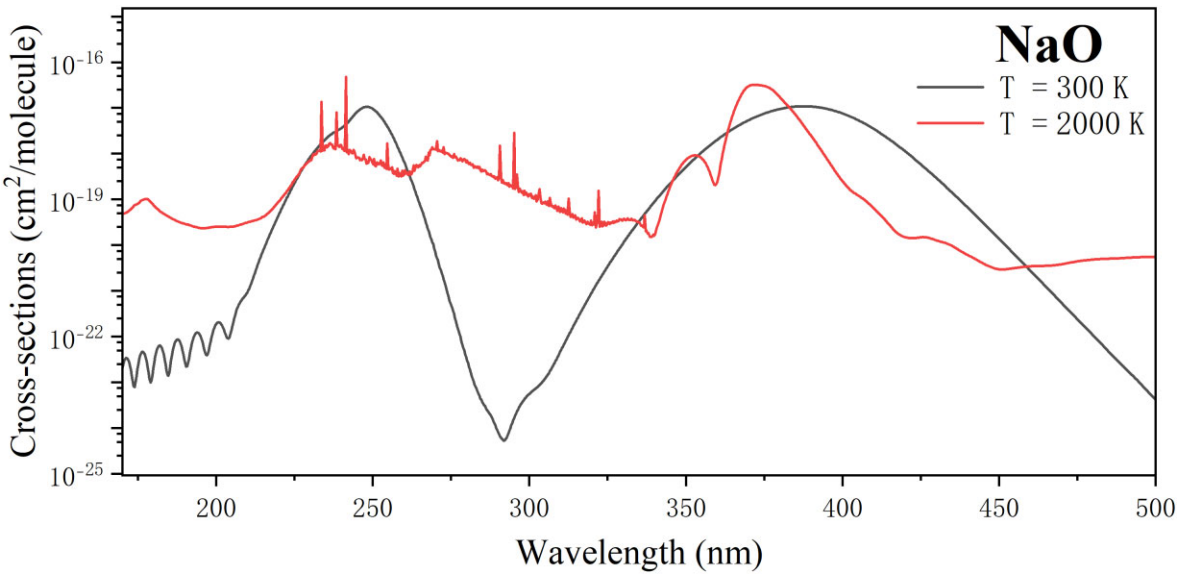

Figure 13. NaO spectrum overview (Bai et al. 2023).

Water is a key molecule in many exoplanetary atmospheres and use of these cross-sections has already shown important effects in models of potentially habitable exoplanets (Ranjan et al. 2020; Broussard et al. 2024).

2.3 Larger molecules

2.3.1 C_2H_2 (EXACT) (Fleury et al. 2025)

Photodissociation cross-sections for acetylene (C_2H_2) were experimentally measured by Fleury and co-workers. The data span a wavelength range from 116 to 228 nm, with a resolution of 0.02 nm. Cross-sections were provided for temperatures ranging from 296 to 773 K under a pressure of 1 bar, see Fig. 18. These cross-sections have been used to investigate their impact on exoplanet atmospheres (Fleury et al. 2025).

2.3.2 H_2CO (DTU) (Fateev et al., private communication)

Photodissociation cross-sections for formaldehyde (H_2CO) were experimentally measured by DTU in the far-UV range. The data span a wavelength range from 110 to 230 nm with a resolution of 0.015 nm. Cross-sections were provided for multiple temperatures, 303.15 K, 353.15 K, 423.15 K, and 573.15 K under pressure of 1 bar. They are illustrated in Fig. 19.

2.3.3 NH_3 (DTU)(Fateev et al., private communication)

Photodissociation cross-sections for ammonia (NH_3) were measured experimentally by DTU in the far-UV range. The cross-sections span a wavelength range from 113 to 202 nm, with a resolution of 0.015 nm. Data were provided for two temperatures, 289 K and 295.55 K under pressure of 1 bar, see Fig. 20.

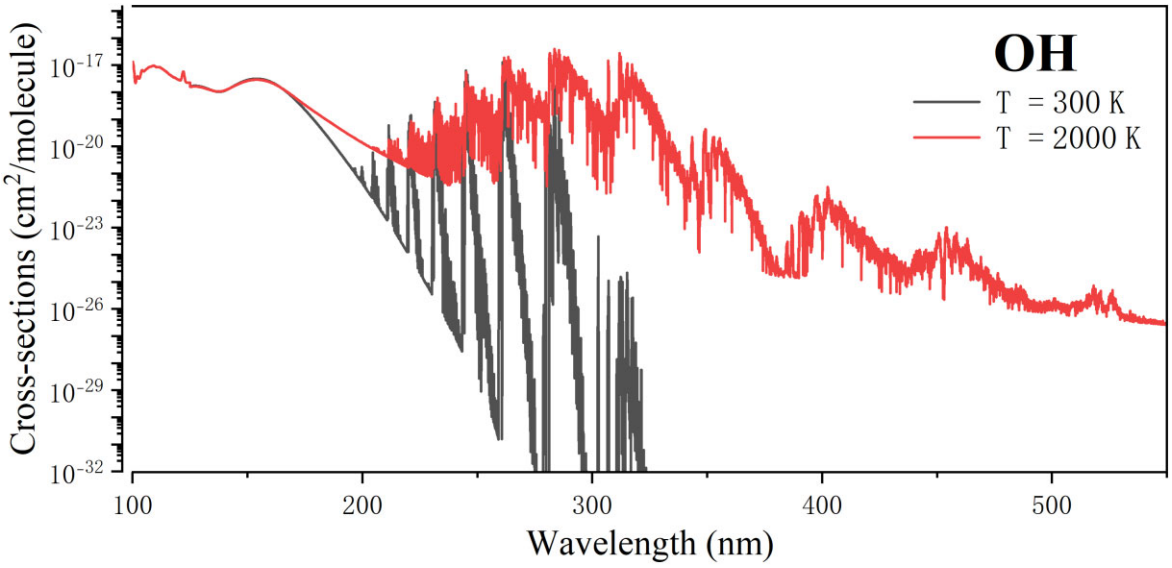

Figure 14. OH spectrum overview (Mitev et al. 2025b).

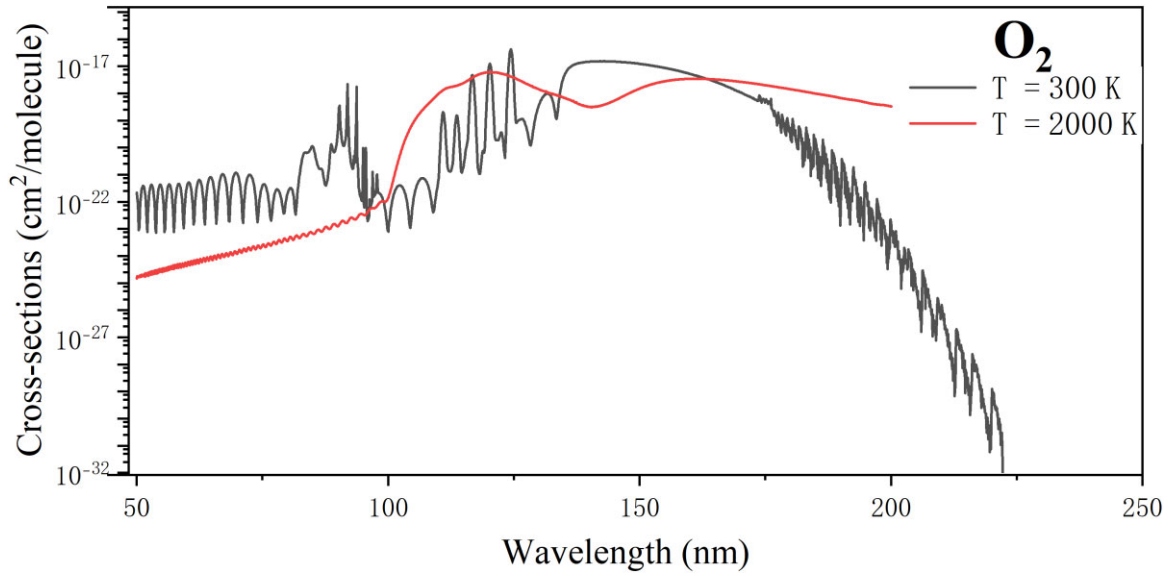

Figure 15. O_2 spectrum overview (Qin et al. 2023).

Additional NH_3 cross-sections up to 573 K will be published soon (Fleury et al., in preparation) and will be available via the EXACT data base.

2.3.4 C_2H_4 (DTU)(Fateev et al., private communication)

Photodissociation cross-sections for ethylene (C_2H_4) were experimentally measured by DTU in the far-UV range. The data span a wavelength range from 113 to 201 nm, with a resolution of 0.065 nm. cross-sections were provided for a single temperature of 562.15 K under pressure of 1 bar, see Fig. 21.

3 DATA BASE STRUCTURE

Access to the data base is implemented using the Django web framework (Holovaty and Willison 2008), which is written in the Python programming language. The data structure of EXOPHOTO is an extension of the original EXOMOL data structure as anticipated by Tennyson et al. (2023). This structure is designed to give a full description of the meta-data for each file and in such a manner that it can be routinely used for both downloading and updating data employing an API (application program interface), see Tennyson et al. (2024). Table 2 provides a specification summary of photodissociation data base. The file types constituting the data base are described in detail below.

3.1 File naming convention

The file naming convention in the EXOPHOTO data base ensures unique, descriptive, and machine-readable file names for each molecular isotopologue.

Files with the extensions `.json` and `.model` include only the 'common part', which consists of the isotopologue's Iso-slug

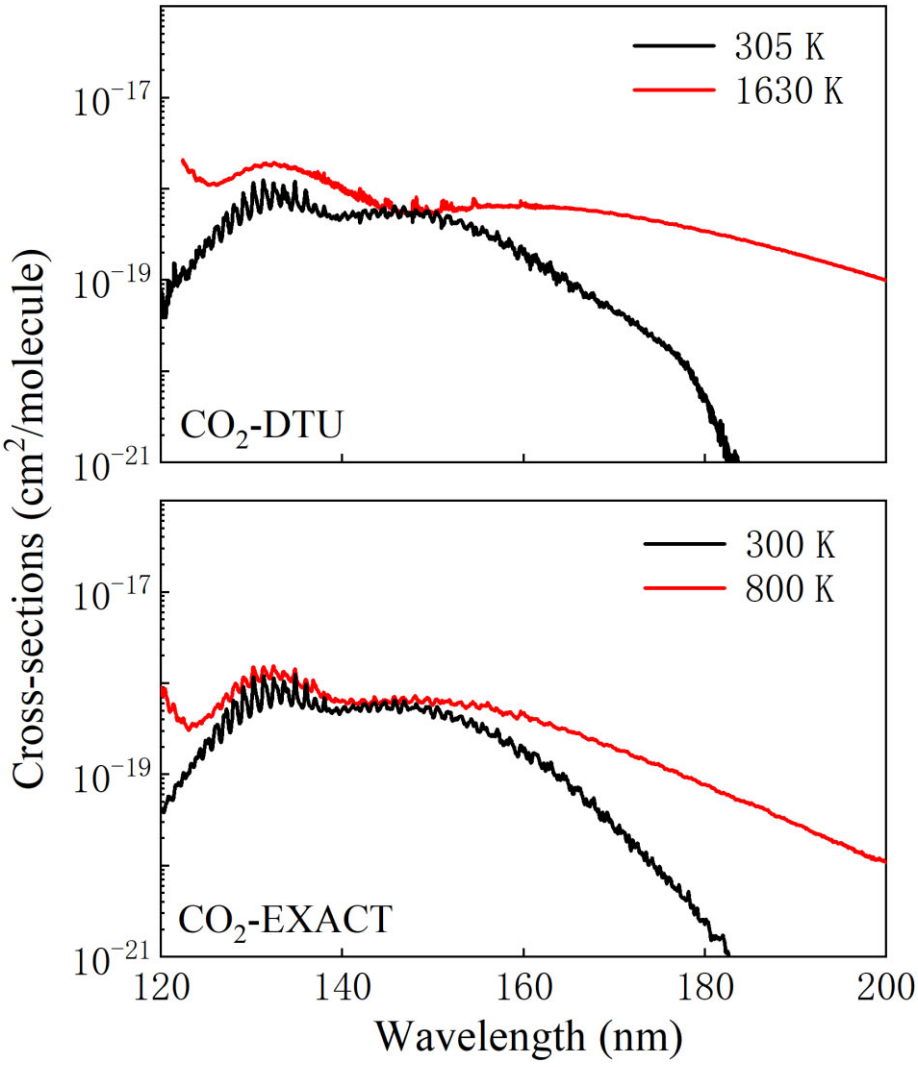

Figure 16. CO_2 spectrum overview from DTU and EXACT (Venot et al. 2018) (Fateev et al., private communication).

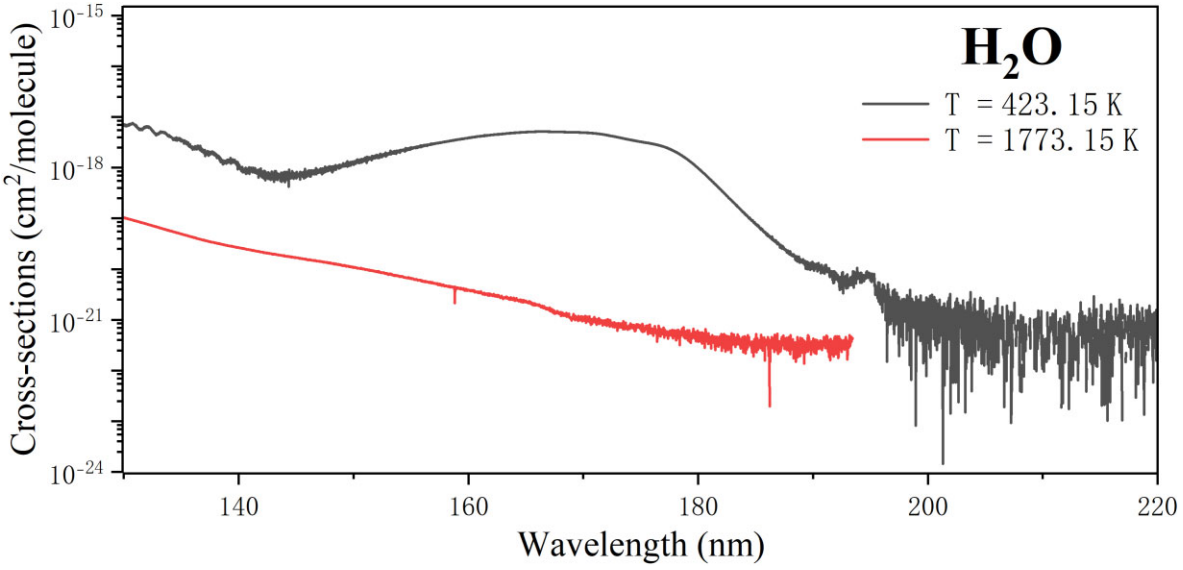

Figure 17. H_2O spectrum overview (Fateev et al., private communication).

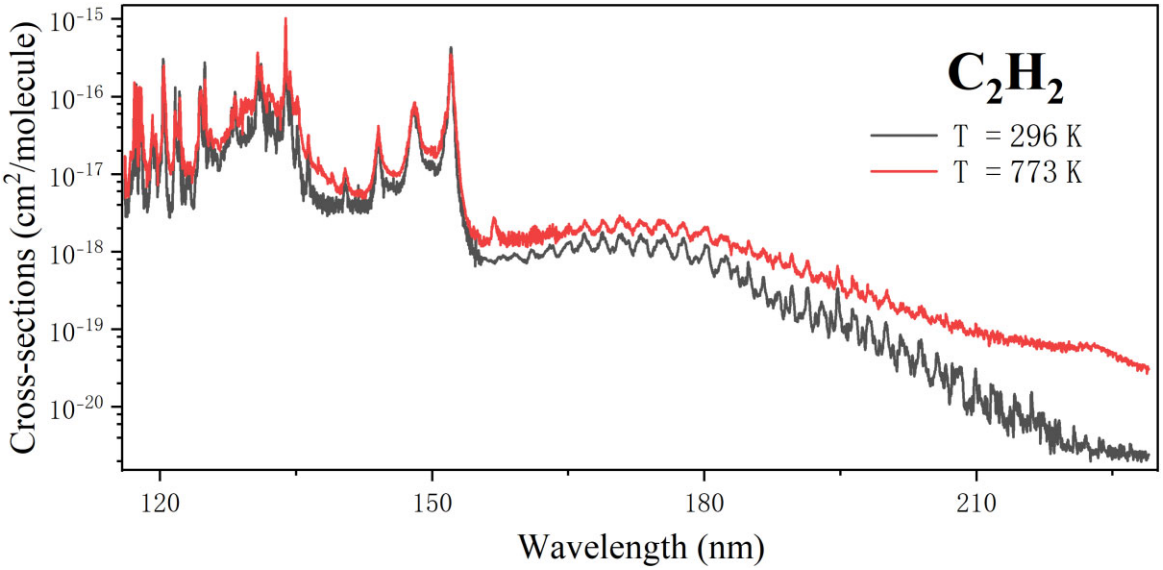

Figure 18. C_2H_2 from EXACT spectrum overview (Fleury et al. 2025).

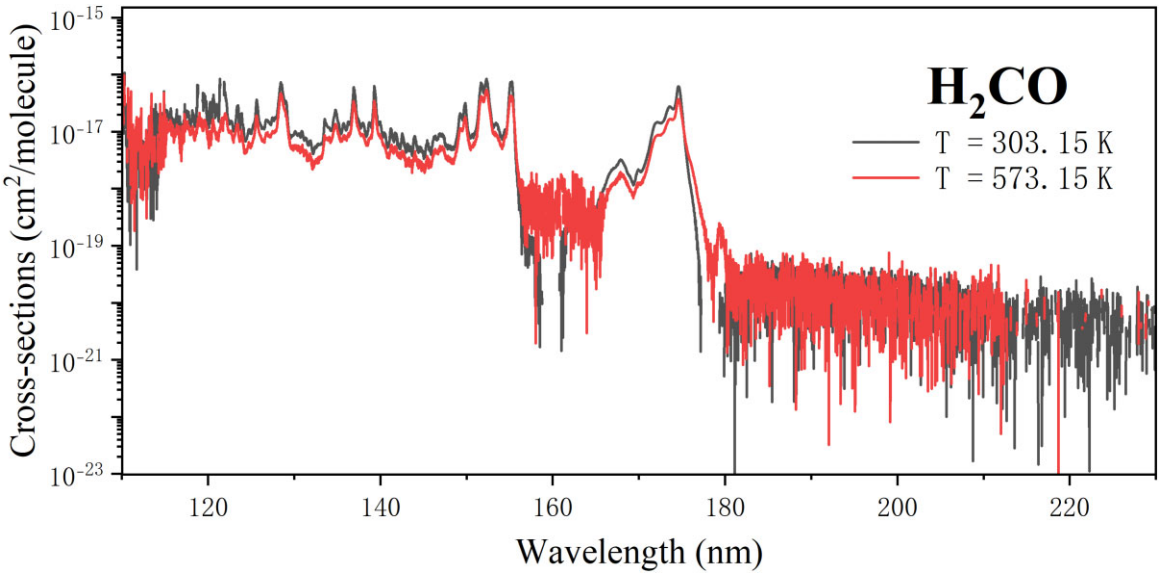

Figure 19. H_2CO spectrum overview (Fateev et al., private communication).

followed by the data set identifier (DATA SET_NAME). The Iso-slug is a plain ASCII-text, XML-safe identifier unique to each isotopologue. For instance, the isotopologue $^1H^{35}Cl$ is represented by the Iso-slug `1H-35Cl`. Following the Iso-slug is the data base resource identifier, indicated by the 'FILE_EXTENSIONS' column in Table 2. This identifier reflects specific data sets associated with the isotopologue. For example, there are two independent photodissociation cross-section sets available for $^1H^{35}Cl$ which are distinguished by the identifiers `PTY` and `PhoMol`. Thus, file names for different types of data associated with each isotopologue follow the general pattern: `<iso_slug>__<data set_name>`, such as `1H-35Cl__PTY`. The data set identifiers currently in use within `ExoPHOTO` include: `PTY` and `MYTHOS` for data from `ExoMol`, `PhoMol`, `UGAMOP`, `DTU`, and `EXACT`.

For photodissociation cross-section files with the extension.photo, additional information is appended to the common part to indicate specific details of the data set. The.photo file names contain a wavelength range (nm), representing the full coverage of the photodissociation process, followed by the temperature in Kelvin (K), pressure in bar, and the binning interval (nm), for which the cross-sections have been computed, after the common part. The naming structure for these files is as follows: `<iso_slug>__<data set_name>__[MINwavelength]-[MAXwavelength]__[Temperature]__[Pressure]__[Delta_wavelength].photo`.

For example, a file representing cross-section data for $^1H^{35}Cl$ at a temperature of 100 K, pressure of 0 bar, with a wavelength range from 100 to 400 nm and a grid of 0.1 nm, would be named `1H-35Cl__PTY__100.0-400.0__0100__0__0.1.photo`. We note that so far none of the calculated cross-sections make any allowance for pressure effects and therefore provide the photodissociation cross-sections at zero pressure; it is not expected that the photodissociation cross-sections will show significant pressure dependence.

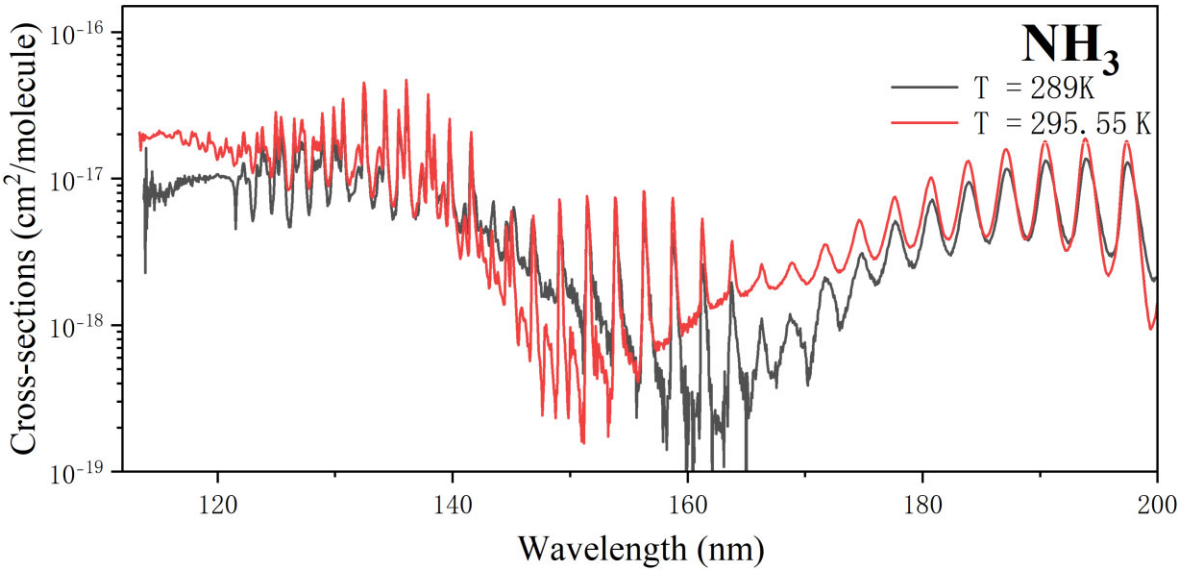

Figure 20. NH_3 spectrum overview (Fateev et al., private communication).

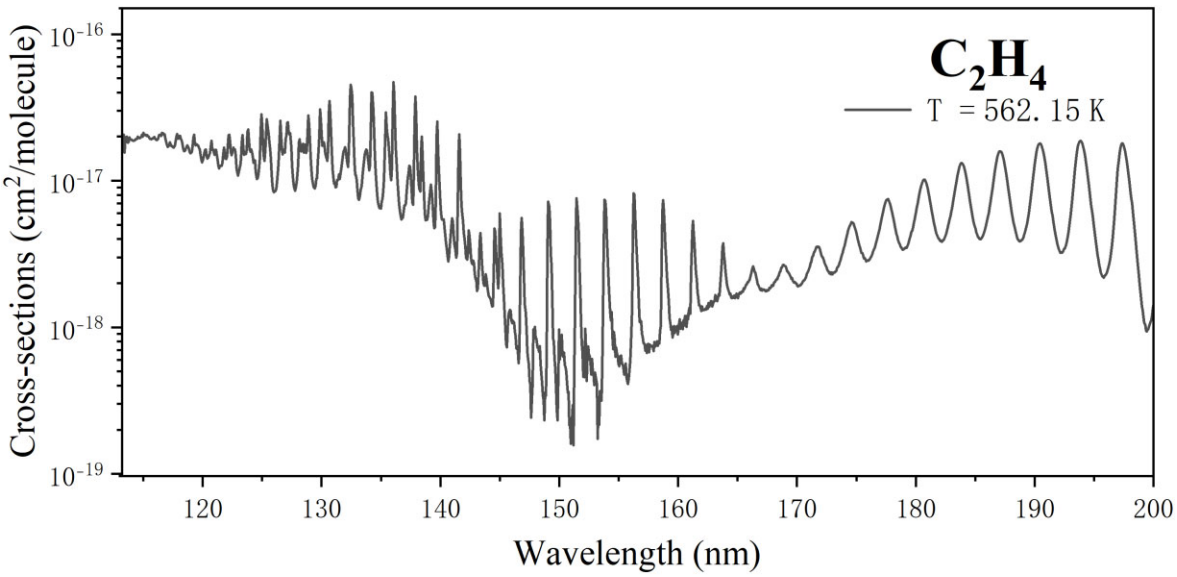

Figure 21. C_2H_4 spectrum overview (Fateev et al., private communication).

Table 2. Specification of the ExoPhoto data base file types. There is a single master file describing the recommended data for N_{mol} molecules which comprise N_{iso} per molecule.

File extension	N_{files}	File Type	Contents
.all	1	Master	Single file defining contents of the ExoPhoto data base
.pdef.json	N_{tot}	Definition	Defines contents of other files for each isotopologue
.model	N_{iso}	Model	Model specification for each isotopologue
.photo	a	Photodissociation cross-sections	Photodissociation temperature-dependent cross sections (wavelength, nm) in.photo format for each isotopologue

N_{mol}: number of molecules in the data base
N_{tot}: total number of.json files, summed across all molecules
N_{iso}: number of isotopologues considered for each molecule
There are N_{tot} sets of.json files, one for each isotopologue
a: number of temp-dependent isotopologues files summed over N_{tot}

Table 3. A general two-column structure of the `.photo` file.

Field	Fortran format	C Format	Description
Wavelength (λ)	`F12.6`	`%12.6f`	Wavelength, in nm
Total (σ)	`ES14.8`	`%14.8e`	Total cross section, in cm^2 per molecule

Table 4. Example of a multicolumn structure of the `.photo` file in ExoPhoto for CS, containing total as well as partial cross-sections for individual final electronic states of the system.

Field	Fortran format	C Format	Description
Wavelength (λ)	`F12.6`	`%12.6f`	Wavelength, in nm
Total (σ)	`ES14.8`	`%14.8e`	Total cross section, in cm^2 per molecule
$2\,^1\Pi$	`ES14.8`	`%14.8e`	Cross section for the $2\,^1\Pi$ state, in cm^2 per molecule
$A'\,^1\Sigma^+$	`ES14.8`	`%14.8e`	Cross section for the $A'\,^1\Sigma^+$ state, in cm^2 per molecule
$3\,^1\Pi$	`ES14.8`	`%14.8e`	Cross section for the $3\,^1\Pi$ state, in cm^2 per molecule
$B'\,^1\Sigma^+$	`ES14.8`	`%14.8e`	Cross section for the $B'\,^1\Sigma^+$ state, in cm^2 per molecule
$4\,^1\Pi$	`ES14.8`	`%14.8e`	Cross section for the $4\,^1\Pi$ state, in cm^2 per molecule
$A\,^1\Pi$	`ES14.8`	`%14.8e`	Cross section for the $A\,^1\Pi$ state, in cm^2 per molecule

3.2 Photodissociation cross-section file

Photodissociation cross-sections are stored in ExoPhoto files with the extension `.photo`. The primary columns include the wavelength (column 1, λ, in nm) and the total photodissociation cross-section (column 2, σ, in cm^2 per molecule). Additional columns, if applicable, provide partial cross-sections for individual final electronic states of the system (e.g. $2\,^1\Pi$, $A'\,^1\Sigma^+$). The fields are separated by a single space and the partial cross-sections sum to give the total cross-section.

The photodissociaition cross-sections provided by ExoPhoto are temperature- and in some cases, pressure-dependent. Each `.photo` file provides data for a single combination of temperature and pressure. The corresponding temperatures and pressures are indicated in the file header, which specifies the temperature (in K) and the pressure (in bar) under which the cross-sections were determined.

The Fortran format for the complete `.photo` file is defined as `(F12.6, 1x, ES14.8)`, where each cross-section field is separated by a single space. This file structure allows for representation of wavelength-dependent photodissociation data for various isotopologues, with all other information encoded in the file names and the directory structure.

3.2.1 Two-column data set

For most molecules, only two columns are provided: wavelength and total cross-section, see Table 3.

3.2.2 Multiple column data set

However, as noted above, for certain molecules such as CS and MgH, the cross-section data are further divided by outgoing channels, extra columns are provided corresponding to different dissociating final states. For example, the `.photo` file format of CS molecule is shown in Table 4. These channels are specified in the `.pdef.json` definition file of the relevant isopotopologue.

3.3 The definition file

The core information about each isotopologue is contained within its JSON definition file. JSON (JavaScript Object Notation) is a lightweight, human-readable data-interchange format commonly used for organizing and transmitting structured data (Pezoa et al. 2016).

In this case, the `.pdef.json` definition file adheres to the ExoPhoto format `<iso_slug>__<data set_name>.pdef.json`. This file specifies the data available from ExoPhoto for a given isotopologue and describes potential applications of the data.

Within this format, information provided is grouped into several main sections (highlighted in bold in Table 5), with each section describing a specific characteristic or property of the molecule. Each main section may contain multiple subsections that further detail aspects of that category.

For some isotopologues, the JSON files also contain information about different photodissociation channels, providing data on branching ratios or quantum yields. In photodissociation studies, according to IUPAC (2006) and Braslavsky (2007), a channel refers to a specific dissociation pathway characterized by distinct photofragments or electronic states. The branching ratio describes how the total photodissociation yield is distributed among various channels, effectively indicating the fraction of dissociation events occurring via each specific channel. By contrast, the quantum yield provides a measure of the overall efficiency of the photodissociation process, defined as the total number of dissociation events per photon absorbed, regardless of the channel involved. Thus, branching ratios detail the internal distribution among dissociative channels, while quantum yields quantify the global efficiency of photodissociation.

Appendix A presents the definition file `.pdef.json` for the $^{12}C^{32}S$ molecule from the photodissociation data set UGAMOP-CS, as a typical example. These standardized fields allow consistent identification and reference across various isotopologues.

The definition file serves following purposes.

3.3.1 Standardized ExoPhoto file usage

The data set format used in this data base follows ExoMol standards, designed to provide comprehensive photodissociation cross-section data for a given isotopologue. Each isotopologue is described by fields such as the isotopologue formula (`iso_formula`), the simplified slug name (`iso_slug`), InChIKey (`inchikey`), InChI string (`inchi`), and molecular mass in Daltons (`mass_in_Da`). These standardized fields allow consistent identification and reference across various isotopologues.

Table 5. Definition of the.pdef.json file format; each entry starts on a new line.

Field	Fortran Format	C Format	Description
Header Information			
iso_formula	A27	%27s	Isotopologue chemical formula
iso_slug	A160	%160s	Isotopologue identifier (constructed from isotopic composition and element symbol)
inchikey	A27	%27s	InChIKey identifier for the molecule
inchi	A20	%20s	Standard InChI representation for the molecule
mass_in_Da	F12.6	%12.6f	Molecular mass in Daltons (Da)
Data set Information			
name	A10	%10s	Name of the resource data set
version	I8	%8d	Version of the data set (format: YYYYMMDD)
max_temperature	F8.2	%8.2f	Maximum temperature in data set for photodissociation cross-sections
min_wavelength	F8.2	%8.2f	Minimum wavelength in data set (nm)
max_wavelength	F8.2	%8.2f	Maximum wavelength in data set (nm)
Units			
units.T	A2	%2s	Temperature unit (K)
units.p	A3	%3s	Pressure unit (bar)
units.w	A3	%3s	Wavelength unit (nm)
Columns Information			
Wavelength	A10	%10s	First column: Wavelength (nm)
Total	A10	%10s	Second column: Total photodissociation cross section (cm^2 per molecule)
Channel	A10	%10s	Subsequent columns: cross section per channel (cm^2 per molecule)
File Information			
files.p	I3	%3d	Pressure (bar)
files.T	F6.2	%6.2f	Temperature (K)
files.delta_wavelength	F4.1	%4.1f	Wavelength interval (nm)
files.nlines	I6	%6d	Number of lines in the file
files.filename	A40	%40s	Filename for photodissociation cross-section file (constructed from parameters)

Table 6. InChI and InChIKey for General HCl and Specific Isotopologues (NIST 2023; InChI Trust 2024)

Description	InChI	InChIKey
General HCl (average molecular weight: 36.46 Da)	1S/ClH/h1H	VEXZGXHMUGYJMC-UHFFFAOYSA-N
$^{1}H-{}^{35}Cl$	1S/ClH/h1H/i1+0	VEXZGXHMUGYJMC-UHFFFAOYSA-N
$^{1}H-{}^{37}Cl$	1S/ClH/h1H/i1+0;2+0	VEXZGXHMUGYJMC-NJFSPNSNSA-N
$^{2}H-{}^{35}Cl$ (DCl)	1S/ClH/h1H/i1+1	VEXZGXHMUGYJMC-DYCDLGHISA-N
$^{2}H-{}^{37}Cl$	1S/ClH/h1H/i1+1;2+0	VEXZGXHMUGYJMC-DQGQKLTASA-N

The InChI encodes detailed structural information, such as the connectivity of atoms and the presence of hydrogen. The InChIKey, a hashed version of the InChI, is a compact, fixed-length string designed for easier indexing and searching. The process of generating an InChIKey involves applying a hashing algorithm to the full InChI string. This algorithm compresses the detailed structural information into a unique 27-character alphanumeric code, divided into three blocks separated by hyphens: the first block encodes the connectivity, the second encodes additional structural features, and the third indicates the version and checksum of the key. Both identifiers ensure consistency and compatibility across data bases (Heller & McNaught 2015).

For the general species HCl, the InChI represents the molecule as a collection of isotopologues, defined by the averaged molecular weight of 36.46 Da. This molecular weight reflects the natural abundance of its isotopes ^{1}H, ^{2}H, ^{35}Cl, and ^{37}Cl. The InChI for this 'average' HCl is 1S/ClH/h1H, and the corresponding InChIKey is VEXZGXHMUGYJMC-UHFFFAOYSA-N. However, this representation does not account for specific isotopic compositions. To distinguish specific isotopologues, an isotopic layer is added to the InChI string (NIST 2023).

The four major isotopologues of HCl are $^{1}H^{35}Cl$, $^{1}H^{37}Cl$, $^{2}H^{35}Cl$ (DCl), and $^{2}H^{37}Cl$. Each isotopologue has a unique InChI and InChIKey, reflecting its specific isotopic composition. Table 6 summarizes the InChI and InChIKey representations for both general HCl and its specific isotopologues as illustrated in Table 6.

While InChIKeys are highly standardized, they are not always unique in cases, such as stereoisomers or isotopic variations (Heller & McNaught 2015; InChI Trust 2024). This is why additional fields like the isotopologue slug (iso_slug) or molecular mass in Daltons (mass_in_Da) are included for more precise identification in data bases.

3.3.2 *Improved data base functionality*

The data set includes photodissociation cross-section (photodissociation_xsecs) data, with detailed fields for maximum temperature (max_temperature), wavelength range (min_wavelength, max_wavelength), and units for key parameters. This information facilitates data base operations like sorting, filtering, and selecting based on temperature, pressure, and wavelength increment values, as stored in the files section. Each entry in files specifies conditions such as pressure (p), temperature (T), and wavelength increment (delta_wavelength), with filenames indicating all these parameters.

Table 7. Extract from the ExoPhoto Master file showing the overall header and information contained for HCl

Field	Description
exophoto.master	ID
20241225	Version number with format YYYYMMDD
20	Number of molecules in the data base
28	Number of isotopologues in the data base
5	Number of data sets in the data base
Molecule information	
Molecule Name	The common name of the molecule (`HCl`)
Chemical Formula	The chemical formula of the molecule
Number of Isotopologues	Total number of isotopologues available for `HCl`
Data bases	The data bases where `HCl` isotopologues are listed
Isotopologue overview	
`1H-35Cl`	Found in `PTY` and `PHOTO-PhoMol_HCl` data bases
`2H-35Cl`	Found only in the `PTY` data base
`1H-37Cl`	Found only in the `PTY` data base
`2H-37Cl`	Found only in the `PTY` data base
Isotopologue details	
Inchi Key	The InChIKey identifier for the isotopologue
Iso-slug	The isotopologue slug
IsoFormula	The isotopologue formula in a standardized format
Data set Name	The data set where the isotopologue data is available
Version Number	Version of the data set containing isotopologue information

3.3.3 Facilitated updates

Each data set is version-controlled, indicated by the `version` field in the date format `YYYYMMDD`. This versioning supports easy updating of isotopologue data, allowing users to check for newer versions of specific data sets and automatically download modified files. This feature ensures up-to-date data usage without requiring code modifications (Tennyson et al. 2023).

3.4 Spectroscopic model file

Each calculated data set in ExoPhoto is based on a well-developed and comprehensive spectroscopic model for the specified isotopologue; as far as possible in the ExoMol/ExoPhoto data base the actual data provided is supplemented by detailed specification of the spectroscopic model used. This takes the form of reference to the original paper in all cases and provision of input files used and code specification for the calculations where possible. In practice, at present it is only ExoMol data for which we are able to provide the full spectroscopic model.

For the $^1H^{35}Cl$ isotope of HCl, ExoMol provides spectroscopic data available on the website in the form of a corresponding model file. Appendix B shows the `.model` file for the $^1H^{35}Cl$ molecule, which also serves as an input file for the code Duo (Yurchenko et al. 2016).

3.5 The master file

A master summary file, named `exophoto.all.json`, consolidates the contents of the whole data base. This file, which is available at www.exomol.com/exophoto.all.json, provides a computer readable (JSON format) list of recommended data sets, including those for each isotopologue under the ExoPhoto structure. The `master` file provides a summary of the data base's contents and ensures easy access to the current version number of each data set, enabling users to efficiently track updates. The file begins with general statistics about the data base, including the total number of molecules, isotopologues, and data sets. Specifically, this data base currently contains 20 molecules, 28 isotopologues, and data are taken from a total of five projects/data bases.

For each molecule, the file includes its names, chemical formula, and the number of associated isotopologues. An example of the ExoPhoto master file for HCl is given in the Appendix C, illustrating the common uniform structure used for all molecules, with differences only in specific data values; isotopologue-specific details are also provided, including unique identifiers such as InChI keys, iso-slugs, isotopic formulas, data set names, and version numbers (see Appendix C). The format of the `ExoPhoto.master.json` file is illustrated in Table 7.

4 CONCLUSIONS

The ExoPhoto data base is an extension of the ExoMol data base, specifically developed to address the need for high-accuracy photodissociation cross-section data for molecules of astronomical interest. ExoPhoto currently includes 12 molecules derived from theoretical models provided by three theoretical data bases and eight molecules supported by experimental data from including two from the experimental EXACT data bases. These cross-sections are clearly only a subset of those needed to model photon-driven chemistries at the top exoplanetary atmospheres and elsewhere. We are currently working on photodissociation for a number of diatomic molecules and expanding our treatment to triatomics with initial focus on HCN and H_2S.

An important future development of the ExoPhoto data base will be the inclusions of non-local thermodynamic equilibrium (non-LTE) cross sections i.e. cross-sections which are resolved according to the initial states of the target molecule. As the number of initial states can be very large, particularly for polyatomic molecules, this step will lead to a huge expansion in the size of the data base and therefore needs to be approached with some care. At present we are using OH as a prototype to understand how users will utilize non-LTE photodissociation data. Initial state specified OH photodissociation cross-sections suitable for non-LTE studies are available on request.

Currently those molecules for which branching ratios, where available, are given in terms of partial cross-section for the outgoing

electronic state. In future we aim to correlate these outgoing final states with specific states of the asymptotic fragments, for example diatomic states we would provide information on the atomic states formed. This will provide a more comprehensive description but is not entirely straightforward as the available partial cross-sections contain some cross-sections to states which actually only dissociate after undergoing a state crossing to another (currently unspecified) dissociative state.

The DTU team aims to extend their data sets by photoabsorption cross-section measurements of molecules relevant to various industrial applications [e.g. Carbon Capture Utilization and Storage (CCUS), H_2 and biogas production, transportation, and storage]. The molecules of interest are: HCl, Cl_2, H_2S, NH_3, CO_2, CO, O_2, H_2O, etc. The measurements will first be performed at ambient conditions (about 298 K and 1 atm), then at elevated pressures (at 298 K), and finally at elevated pressures and temperatures (up to 100 atm and 1300 K). The measurements will be conducted in the 110–240 nm spectral range using primary reference materials (gas mixtures).

ACKNOWLEDGEMENTS

This work was supported by the European Research Council (ERC) under the European Union's Horizon 2020 research and innovation programme via Advanced Grant 883830 and the STFC Project No. ST/Y001508/1. OV acknowledges funding from Agence Nationale de la Recherche (ANR), project 'EXACT' (ANR-21-CE49-0008-01) as well as from the Centre National d'Études Spatiales (CNES).

CONFLICT OF INTEREST

Authors declare no conflict of interest.

DATA AVAILABILITY

All the data discussed in this paper are available from the ExoPhoto website https://exomol.com/exophoto/ except for non-LTE cross-sections for OH which can be obtained on request from the corresponding author.

REFERENCES

Albert D. et al., 2020, Atoms, 8, 76
Badhan M. A., Wolf E. T., Kopparapu R. K., Arney G., Kempton E. M.-R., Deming D., Domagal-Goldman S. D., 2019, ApJ, 887, 34
Bai T., Qin Z., Liu L., 2021, MNRAS, 505, 2177
Bai T., Yang X., Qin Z., Liu L., 2023, MNRAS, 527, 3847
Bowesman C. A., Akbari H., Hopkins S., Yurchenko S. N., Tennyson J., 2022, J. Quant. Spectrosc. Radiat. Transfer, 289, 108295
Braslavsky S. E., 2007, Pure Appl. Chem., 79, 293
Broussard W., Schwieterman E. W., Ranjan S., Sousa-Silva C., Fateev A., Reinhard C. T., 2024, ApJ, 967, 114
Dubernet M.-L. et al., 2016, J. Phys. B: Atomic, Molecular and Optical Physics, 49, 074003
Fleury B., Gudipati M. S., Henderson B. L., Swain M., 2019, ApJ, 871, 158
Fleury B. et al., 2025, A&A, 693, A82
Gay C., Abel N., Porter R., Stancil P., Ferland G. J., Shaw G., Van Hoof P., Williams R., 2012, ApJ, 746, 78
Heays A. N., Bosman A. D., van Dishoeck E. F., 2017, A&A, 602, A105
Heller S. R., McNaught A. D., Pletnev I., Stein S., Tchekhovskoi D., 2015, J. Cheminfo., 7, 23
Holovaty A., Willison S., 2008, Django web framework. Django Software Foundation, USA, http://www. djangoproject.com (Accessed November 2024)
Hrodmarsson H. R., Van Dishoeck E. F., 2023, AA, 675, A25
Huebner W. F., Mukherjee J., 2015, Planet. Space Sci., 106, 11
InChI Trust, 2024, Inchi software downloads. InChI Trust Limited, Cambridge (Accessed November 2024)
International Union of Pure and Applied Chemistry, 2006, Compendium of Chemical Terminology (the 'gold book'): branching fraction, 2nd edn. International Union of Pure and Applied Chemistry, North Carolina, https://doi.org/10.1351/goldbook.B00725 (Accessed November 2024)
Keller-Rudek H., Moortgat G. K., Sander R., Sörensen R., 2013, Earth Syst. Sci. Data, 5, 365
Lewis N. K. et al., 2020, ApJ, 902, L19
Mitev G. B., Yurchenko S. N., Tennyson J., 2024, J. Chem. Phys., 160, 144110
Mitev G. B., Bowesman C. A., Zhang J., Yurchenko S. N., Tennyson J., 2025a, MNRAS, 536, 3401
Mitev G. B., Pezzella M., Bowesman C. A., Zhang J., Yurchenko S. N., Tennyson J., 2025b, MNRAS, 539, 3732
Miyake S., Gay C., Stancil P., 2011, ApJ, 735, 21
NIST, 2023, The IUPAC International Chemical Identifier (InChI). National Institute of Standards and Technology, Gaithersburg, MD, https://webbook.nist.gov/cgi/inchi/InChI%3D1S/ClH/h1H
Pattillo R. J., Cieszewski R., Stancil P. C., Forrey R. C., Babb J. F., McCann J. F., McLaughlin B. M., 2018, ApJ, 858, 10
Pavlenko Y., Tennyson J., Yurchenko S. N., Schmidt M. R., Jones H. R. A., Lyubchik Y., Suárez Mascareño A., 2022, MNRAS, 516, 5655
Pezoa F., Reutter J. L., Suarez F., Ugarte M., Vrgoč D., 2016, in Proc. 25th International Conference on World Wide Web. Association for Computing Machinery, New York, p. 263
Pezzella M., Yurchenko S. N., Tennyson J., 2021, Phys. Chem. Chem. Phys., 23, 16390
Pezzella M., Yurchenko S. N., Tennyson J., 2022, MNRAS, 514, 4413
Pezzella M., Mitev G., Yurchenko S. N., Tennyson J., Mitrushchenkov A. O., 2024, Phys. Chem. Chem. Phys., 26, 27519
Qin Z., Bai T., Liu L., 2021a, MNRAS, 508, 2848
Qin Z., Bai T., Liu L., 2021b, ApJ, 917, 87
Qin Z., Bai T., Liu L., 2022a, MNRAS, 510, 3011
Qin Z., Bai T., Liu L., 2022b, MNRAS, 516, 550
Qin Z., Hu P., Bai T., Liu L., 2023, ApJS, 269, 48
Ranjan S., Schwieterman E. W., Harman C., Fateev A., Sousa-Silva C., Seager S., Hu R., 2020, ApJ, 896, 148
Schinke R., 1993, Photodissociation Dynamics. Cambridge Univ. Press
Stibbe D. T., Tennyson J., 1998, New J. Phys, 1, 2
Tennyson J., Yurchenko S. N., 2012, MNRAS, 425, 21
Tennyson J., Pezzella M., Zhang J., Yurchenko S. N., 2023, RASTI, 2, 231
Tennyson J. et al., 2024, J. Quant. Spectrosc. Radiat. Transfer, 326, 109083
UGAMOP, Stancil C.P., Libo Z., Benhui Y., Andy O., 2014, Molecular Opacity Project Database. University of Georgia, Athens, https://sites.physast.uga.edu/ugamop/ (Accessed November 2024).
Uhlikova T., Yurchenko S. N., Perri A. N., Tennyson J., Kim G.-S., 2025, J. Chem. Phys., 162, 144108
Valiev R., Berezhnoy A., Sidorenko A., Merzlikin B., Cherepanov V., 2017, Planet. Space Sci., 145, 38
Venot O., Rocchetto M., Carl S., Hashim A. R., Decin L., 2016, ApJ, 830, 77
Venot O. et al., 2018, A&A, 609, A34
Venot O. et al., 2024, EXACT: EXoplanetary Atmospheric Chemistry at High Temperature. Université Paris Cité and Univ Paris-Est Créteil, Paris, France, https://www.anr-exact.cnrs.fr/
Vujčič V., Jevremović D., Mihajlov A., Ignjatović L. M., Srećković V., Dimitrijević M., Malović M., 2015, JApA, 36, 693
Weck P., Schweitzer A., Stancil P., Hauschildt P., Kirby K., 2003a, ApJ, 584, 459
Weck P., Schweitzer A., Stancil P., Hauschildt P., Kirby K., 2003b, ApJ, 582, 1059
Weck P., Stancil P., Kirby K., 2003c, ApJ, 582, 1263
Yurchenko S. N., Lodi L., Tennyson J., Stolyarov A. V., 2016, Comput. Phys. Commun., 202, 262
Yurchenko S. N., Szajna W., Hakalla R., Semenov M., Sokolov A., Tennyson J., Pavlenko Y., Schmidt M. R., 2024, MNRAS, 527, 9736

APPENDIX A: EXAMPLE PDEF.JSON FILE BY CS MOLECULE


```
{
   ‘‘isotopologue": {
        "iso_formula": "(12C)(32S)",
        "iso_slug": "12C-32S",
        "inchikey": "DXHPZXWIPWDXHJ-UHFFFAOYSA-N",
        "inchi": "1S/CS/c1-2",
        "mass_in_Da": 43.972071
    },
    "dataset": {
        "name": "UGAMOP-CS",
        "version": 20240621,
        "photodissociation_xsecs": {
            "max_temperature": 10000.0,
            "min_wavelength": 50.0,
            "max_wavelength": 5000.0,
            "units": {
                "T": "K",
                "p": "bar",
                "dwv": "nm"
            },
            "columns": [
                {"name": "wavelength", "units": "nm"},
                {"name": "Total", "units": "cm2/molecule"},
                {"name": "2(1PI)", "units": "cm2/molecule"},
                {"name": "A’(1SIGMA+)", "units": "cm2/molecule"},
                {"name": "3(1PI)", "units": "cm2/molecule"},
                {"name": "B’(1SIGMA+)", "units": "cm2/molecule"},
                {"name": "4(1PI)", "units": "cm2/molecule"},
                {"name": "A(1PI)", "units": "cm2/molecule"}
            ],
            "files": [
                {
                    "p": 0,
                    "T": 1000,
                    "dwv": 3.33,
                    "nlines": 1500,
                    "filename": "12C-32S__UGAMOP-CS__50.0-5000.0__1000__0__3.33.photo"
                },
                {
                    "p": 0,
                    "T": 2000,
                    "dwv": 3.33,
                    "nlines": 1500,
                    "filename": "12C-32S__UGAMOP-CS__50.0-5000.0__2000__0__3.33.photo"
                },

                ...

                {
                    "p": 0,
                    "T": 10000,
                    "dwv": 3.33,
                    "nlines": 1500,
                    "filename": "12C-32S__UGAMOP-CS__50.0-5000.0__10000__0__3.33.photo"
                }
            ]
        }
    }
}
```

APPENDIX B: EXAMPLE ExoMol SPECTROSCOPIC .model FILE FOR $^{1}H^{35}Cl$

```
**Input Parameters for HCl**

atoms H Cl

molecule HCl

(Total number of states taken into account)
nstates 2

(Total angular momentum quantum - a value or an interval)
jrot 0 - 100

memory 32 GB

(SOLUTIONMETHOD 5POINTDIFFERENCES)

(Defining the integration grid)
grid
  npoints        251    (odd)
  range  0.5,3.00
  type 0   (nsub)
  re 0.9
end

symmetry Cs(M)

**Diagonalizer and Contraction Parameters**

DIAGONALIZER
 SYEV   (SYEVR)
end

CONTRACTION
  vib
  vmax  200
  enermax 150000
END

**Potential Energy Surfaces**

poten 1
name "X 1Sigma+"
symmetry +
type   grid
lambda 0
mult   1
units Angstroms Eh
values
  0.80000001192092896  0.380179974751452 10
  0.82090001180768013  0.336233016344625 99
  ...
end

poten 2
name "3 1Sigma+"
symmetry +
type   grid
lambda 0
mult   1
units Angstroms Eh
values
  0.800000011920929  0.807352361388752
  0.82090001180768   0.76269762315556
  ...
end

```

```
**Intensity Parameters**

INTENSITY
  absorption
  thresh_intes  1e-30
  thresh_line   1e-30
  temperature   10000
  nspin 0.5  1.5
  linelist   3s-x-L3.00-J120
  J,  0.0 - 120
  freq-window        0.0, 1000000.0
  energy low  0., 37239.9374, upper    80000, 1.00E+06
end

**Dipole Moments**

dipole  1 2
name "<3S+ |DMZ|  X1Sigma+ >"
spin   0.0 0.0
lambda  0  0
type   grid
factor   1   (0, 1 or i)
units Angstroms ea0
values
  0.8000        0.4966
  1.0000        0.5004
  1.2750        0.4411
  ...
end
```

APPENDIX C: EXTRACT FROM THE EXOPHOTO MASTER FILE SHOWING THE SPECIFICATIONS FOR THE HCL ISOTOPOLGUES

```
{
  "ExoPhoto": {
    "ID": "exophoto.master.json",
    "version": "20241225"
  },
  "molecules": {
    "HCl": {
      "name": "Hydrogen chloride",
      "ordinary_formula": "HCl",
      "isotopologues": {
        "1H-35Cl": {
          "inchikey": "VEXZGXHMUGYJMC-UHFFFAOYSA-N",
          "iso_formula": "(1H)(35Cl)",
          "datasets": {
            "PTY": {
              "version": 20240916,
              "min_wavelength": { "value": 100, "units": "nm" },
              "max_wavelength": { "value": 400, "units": "nm" },
              "min_temperature": { "value": 0.01, "units": "K" },
              "max_temperature": { "value": 10000, "units": "K" },
              "nfiles": 34
            },
            "PhoMol": {
              "version": 20241001,
              "min_wavelength": { "value": 50, "units": "nm" },
              "max_wavelength": { "value": 500, "units": "nm" },
              "min_temperature": { "value": 0.01, "units": "K" },
              "max_temperature": { "value": 10000, "units": "K" },
              "nfiles": 34
            }
          }
        },
        "2H-35Cl": {
          "inchikey": "VEXZGXHMUGYJMC-UHFFFAOYSA-N",
          "iso_formula": "(2H)(35Cl)",
          "datasets": {
            "PTY": {
              "version": 20240916,
              "min_wavelength": { "value": 100, "units": "nm" },
              "max_wavelength": { "value": 400, "units": "nm" },
              "min_temperature": { "value": 0.01, "units": "K" },
              "max_temperature": { "value": 10000, "units": "K" },
              "nfiles": 34
            }
          }
        }
        // ... other HCl isotopologues ...
      }
    },
    "CS": {
      "name": "Carbon monosulfide",
      "ordinary_formula": "CS",
      "isotopologues": {
        "12C-32S": {
          "inchikey": "UEGCPOVBQZRIBG-UHFFFAOYSA-N",
          "iso_formula": "(12C)(32S)",
          "datasets": {
            "UGAMOP": {
              "version": 20240215,
              "min_wavelength": { "value": 50, "units": "nm" },
              "max_wavelength": { "value": 5000, "units": "nm" },
              "min_temperature": { "value": 1000, "units": "K" },
              "max_temperature": { "value": 10000, "units": "K" },
              "nfiles": 10
            }
          }
        }
      }
    }
    // ... other molecules ...
  }
}
```

This paper has been typeset from a TEX/LATEX file prepared by the author.